CHAPTER 5

LOOP ANTENNAS

5.1 INTRODUCTION

Another simple, inexpensive, and very versatile antenna type is the loop antenna. Loop antennas take many different forms such as a rectangle, square, triangle, ellipse, circle, and many other configurations. Because of the simplicity in analysis and construction, the circular loop is the most popular and has received the widest attention. It will be shown that a small loop (circular or square) is equivalent to an infinitesimal magnetic dipole whose axis is perpendicular to the plane of the loop. That is, the fields radiated by an electrically small circular or square loop are of the same mathematical form as those radiated by an infinitesimal magnetic dipole.

Loop antennas are usually classified into two categories, electrically small and electrically large. Electrically small antennas are those whose overall length (number of turns times circumference) is usually less than about one-tenth of a wavelength ($N \times C < \lambda/10$). However, electrically large loops are those whose circumference is about a free-space wavelength ($C \sim \lambda$). Most of the applications of loop antennas are in the HF (3–30 MHz), VHF (30–300 MHz), and UHF (300–3,000 MHz) bands. When used as field probes, they find applications even in the microwave frequency range.

Loop antennas with electrically small circumferences or perimeters have small radiation resistances that are usually smaller than their loss resistances. Thus they are very poor radiators, and they are seldom employed for transmission in radio communication. When they are used in any such application, it is usually in the receiving mode, such as in portable radios and pagers, where antenna efficiency is not as important as the signal-to-noise ratio. They are also used as probes for field measurements and as directional antennas for radiowave navigation. The field pattern of electrically small antennas of any shape (circular, elliptical, rectangular, square, etc.) is similar to that of an infinitesimal dipole with a null perpendicular to the plane of the loop and with its maximum along the plane of the loop. As the overall length of the loop increases and its circumference approaches one free-space wavelength, the maximum of the pattern shifts from the plane of the loop to the axis of the loop which is perpendicular to its plane.

The radiation resistance of the loop can be increased, and made comparable to the characteristic impedance of practical transmission lines, by increasing (electrically) its perimeter and/or the number of turns. Another way to increase the radiation resistance of the loop is to insert, within its circumference or perimeter, a ferrite core of very high permeability which will raise the magnetic field intensity and hence the radiation resistance. This forms the so-called ferrite loop.

Electrically large loops are used primarily in directional arrays, such as in helical antennas (see Section 10.3.1), Yagi-Uda arrays (see Section 10.3.3), quad arrays (see Section 10.3.4), and so on. For these and other similar applications, the maximum radiation is directed toward the axis of the loop forming an end-fire antenna. To achieve such directional pattern characteristics, the circumference (perimeter) of the loop should be about one free-space wavelength. The proper phasing between turns enhances the overall directional properties.

5.2 SMALL CIRCULAR LOOP

The most convenient geometrical arrangement for the field analysis of a loop antenna is to position the antenna symmetrically on the x-y plane, at $z = 0$, as shown in Figure 5.1(a). The wire is assumed to be very thin and the current distribution is given by

$$I_\phi = I_0 \tag{5-1}$$

where I_0 is a constant. Although this type of current distribution is accurate only for a loop antenna with a very small circumference, a more complex distribution makes the mathematical formulation quite cumbersome.

5.2.1 Radiated Fields

To find the fields radiated by the loop, the same procedure is followed as for the linear dipole. The potential function **A** given by (3-53) as

$$\mathbf{A}(x, y, z) = \frac{\mu}{4\pi} \int_C \mathbf{I}_e(x', y', z') \frac{e^{-jkR}}{R} dl' \tag{5-2}$$

is first evaluated. Referring to Figure 5.1(a), R is the distance from any point on the loop to the observation point and dl' is an infinitesimal section of the loop antenna. In general, the current distribution $\mathbf{I}_e(x', y', z')$ can be written as

$$\mathbf{I}_e(x', y', z') = \hat{\mathbf{a}}_x I_x(x', y', z') + \hat{\mathbf{a}}_y I_y(x', y', z') + \hat{\mathbf{a}}_z I_z(x', y', z') \tag{5-3}$$

whose form is more convenient for linear geometries. For the circular loop antenna of Figure 5.1(a), whose current is directed along a circular path, it would be more convenient to write the rectangular current components of (5-3) in terms of the cylindrical components using the transformation (see Appendix VII)

$$\begin{bmatrix} I_x \\ I_y \\ I_z \end{bmatrix} = \begin{bmatrix} \cos\phi' & -\sin\phi' & 0 \\ \sin\phi' & \cos\phi' & 0 \\ 0 & 0 & 1 \end{bmatrix} \begin{bmatrix} I_\rho \\ I_\phi \\ I_z \end{bmatrix} \tag{5-4}$$

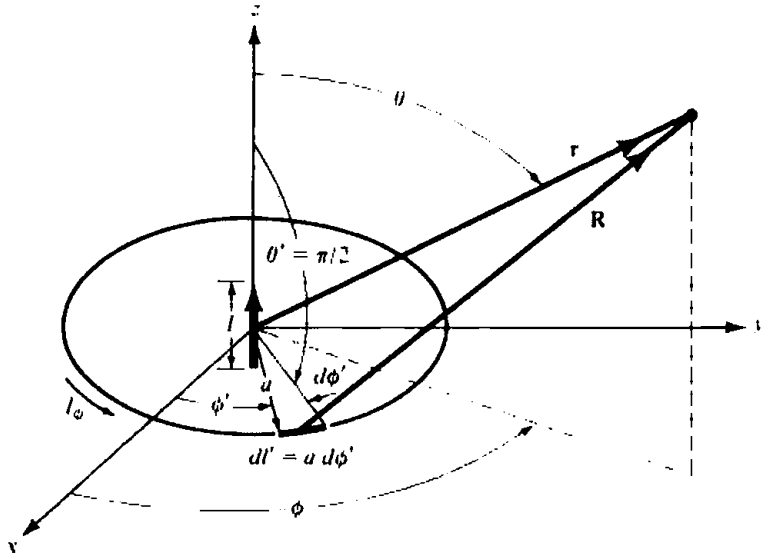

(a) Geometry for circular loop

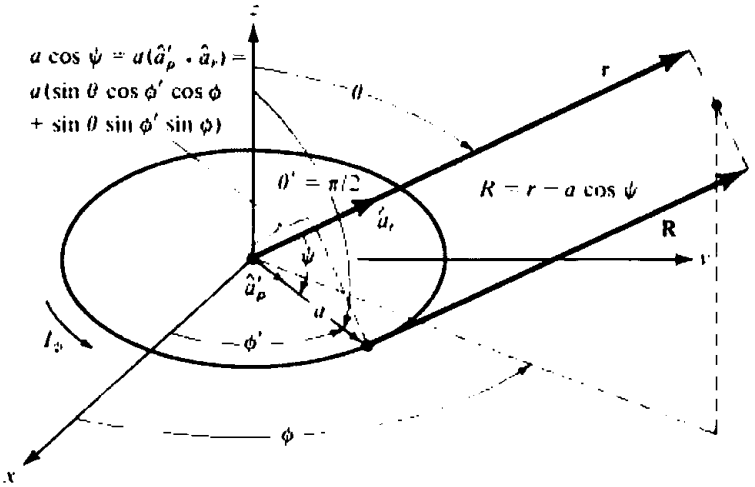

(b) Geometry for far-field observations

Figure 5.1 Geometrical arrangement for loop antenna analysis.

which when expanded can be written as

$$\left.\begin{aligned} I_x &= I_\rho \cos\phi' - I_\phi \sin\phi' \\ I_y &= I_\rho \sin\phi' + I_\phi \cos\phi' \\ I_z &= I_z \end{aligned}\right\} \tag{5-5}$$

Since the radiated fields are usually determined in spherical components, the rectangular unit vectors of (5-3) are transformed to spherical unit vectors using the transformation matrix given by (4-5). That is,

$$\left.\begin{aligned} \hat{\mathbf{a}}_x &= \hat{\mathbf{a}}_r \sin\theta\cos\phi + \hat{\mathbf{a}}_\theta \cos\theta\cos\phi - \hat{\mathbf{a}}_\phi \sin\phi \\ \hat{\mathbf{a}}_y &= \hat{\mathbf{a}}_r \sin\theta\sin\phi + \hat{\mathbf{a}}_\theta \cos\theta\sin\phi + \hat{\mathbf{a}}_\phi \cos\phi \\ \hat{\mathbf{a}}_z &= \hat{\mathbf{a}}_r \cos\theta - \hat{\mathbf{a}}_\theta \sin\theta \end{aligned}\right\} \tag{5-6}$$

Substituting (5-5) and (5-6) in (5-3) reduces it to

$$\begin{aligned}\mathbf{I}_e &= \hat{\mathbf{a}}_r[I_\rho \sin\theta\cos(\phi-\phi') + I_\phi \sin\theta\sin(\phi-\phi') + I_z\cos\theta] \\ &+ \hat{\mathbf{a}}_\theta[I_\rho\cos\theta\cos(\phi-\phi') + I_\phi\cos\theta\sin(\phi-\phi') - I_z\sin\theta] \\ &+ \hat{\mathbf{a}}_\phi[-I_\rho\sin(\phi-\phi') + I_\phi\cos(\phi-\phi')]\end{aligned} \tag{5-7}$$

It should be emphasized that the source coordinates are designated as primed (ρ', ϕ', z') and the observation coordinates as unprimed (r, θ, ϕ). For the circular loop, the current is flowing in the ϕ direction (I_ϕ) so that (5-7) reduces to

$$\mathbf{I}_e = \hat{\mathbf{a}}_r I_\phi \sin\theta\sin(\phi-\phi') + \hat{\mathbf{a}}_\theta I_\phi\cos\theta\sin(\phi-\phi') + \hat{\mathbf{a}}_\phi I_\phi\cos(\phi-\phi') \tag{5-8}$$

The distance R, from any point on the loop to the observation point, can be written as

$$R = \sqrt{(x-x')^2 + (y-y')^2 + (z-z')^2} \tag{5-9}$$

Since

$$\begin{aligned} x &= r\sin\theta\cos\phi \\ y &= r\sin\theta\sin\phi \\ z &= r\cos\theta \\ x^2 + y^2 + z^2 &= r^2 \\ x' &= a\cos\phi' \\ y' &= a\sin\phi' \\ z' &= 0 \\ x'^2 + y'^2 + z'^2 &= a^2 \end{aligned} \tag{5-10}$$

(5-9) reduces to

$$R = \sqrt{r^2 + a^2 - 2ar\sin\theta\cos(\phi-\phi')} \tag{5-11}$$

By referring to Figure 5.1(a), the differential element length is given by

$$dl' = a\,d\phi' \tag{5-12}$$

Using (5-8), (5-11), and (5-12), the ϕ-component of (5-2) can be written as

$$A_\phi = \frac{a\mu}{4\pi}\int_0^{2\pi} I_\phi\cos(\phi-\phi')\frac{e^{-jk\sqrt{r^2+a^2-2ar\sin\theta\cos(\phi-\phi')}}}{\sqrt{r^2+a^2-2ar\sin\theta\cos(\phi-\phi')}}\,d\phi' \tag{5-13}$$

Since the current I_ϕ as given by (5-1) is constant, the field radiated by the loop will not be a function of the observation angle ϕ. Thus any observation angle ϕ can be chosen; for simplicity $\phi = 0$. Therefore (5-13) can be written as

$$A_\phi = \frac{a\mu I_0}{4\pi}\int_0^{2\pi}\cos\phi'\frac{e^{-jk\sqrt{r^2+a^2-2ar\sin\theta\cos\phi'}}}{\sqrt{r^2+a^2-2ar\sin\theta\cos\phi'}}\,d\phi' \tag{5-14}$$

The integration of (5-14) cannot be carried out without any approximations. For small loops, the function

$$f = \frac{e^{-jk\sqrt{r^2+a^2-2ar\sin\theta\cos\phi'}}}{\sqrt{r^2+a^2-2ar\sin\theta\cos\phi'}} \tag{5-15}$$

which is part of the integrand of (5-14), can be expanded in a Maclaurin series in a using

$$f = f(0) + f'(0)\,a + \frac{1}{2!}f''(0)\,a^2 + \cdots + \frac{1}{(n-1)!}f^{(n-1)}(0)\,a^{n-1} + \cdots \tag{5-15a}$$

where $f'(0) = \partial f/\partial a|_{a=0}$, $f''(0) = \partial^2 f/\partial a^2|_{a=0}$, and so forth. Taking into account only the first two terms of (5-15a), or

$$f(0) = \frac{e^{-jkr}}{r} \tag{5-15b}$$

$$f'(0) = \left(\frac{jk}{r} + \frac{1}{r^2}\right) e^{-jkr} \sin\theta \cos\phi' \tag{5-15c}$$

$$f \simeq \left[\frac{1}{r} + a\left(\frac{jk}{r} + \frac{1}{r^2}\right) \sin\theta \cos\phi'\right] e^{-jkr} \tag{5-15d}$$

reduces (5-14) to

$$A_\phi \simeq \frac{a\mu I_0}{4\pi} \int_0^{2\pi} \cos\phi' \left[\frac{1}{r} + a\left(\frac{jk}{r} + \frac{1}{r^2}\right) \sin\theta \cos\phi'\right] e^{-jkr}\, d\phi'$$

$$A_\phi \simeq \frac{a^2\mu I_0}{4} e^{-jkr} \left(\frac{jk}{r} + \frac{1}{r^2}\right) \sin\theta \tag{5-16}$$

In a similar manner, the r- and θ-components of (5-2) can be written as

$$A_r \simeq \frac{a\mu I_0}{4\pi} \sin\theta \int_0^{2\pi} \sin\phi' \left[\frac{1}{r} + a\left(\frac{jk}{r} + \frac{1}{r^2}\right) \sin\theta \cos\phi'\right] e^{-jkr}\, d\phi' \tag{5-16a}$$

$$A_\theta \simeq -\frac{a\mu I_0}{4\pi} \cos\theta \int_0^{2\pi} \sin\phi' \left[\frac{1}{r} + a\left(\frac{jk}{r} + \frac{1}{r^2}\right) \sin\theta \cos\phi'\right] e^{-jkr}\, d\phi' \tag{5-16b}$$

which when integrated reduce to zero. Thus

$$\mathbf{A} \simeq \hat{\mathbf{a}}_\phi A_\phi = \hat{\mathbf{a}}_\phi \frac{a^2\mu I_0}{4} e^{-jkr} \left[\frac{jk}{r} + \frac{1}{r^2}\right] \sin\theta$$

$$= \hat{\mathbf{a}}_\phi j \frac{k\mu a^2 I_0 \sin\theta}{4r} \left[1 + \frac{1}{jkr}\right] e^{-jkr} \tag{5-17}$$

Substituting (5-17) into (3-2a) reduces the magnetic field components to

$$H_r = j\frac{ka^2 I_0 \cos\theta}{2r^2} \left[1 + \frac{1}{jkr}\right] e^{-jkr} \tag{5-18a}$$

$$H_\theta = -\frac{(ka)^2 I_0 \sin\theta}{4r} \left[1 + \frac{1}{jkr} - \frac{1}{(kr)^2}\right] e^{-jkr} \tag{5-18b}$$

$$H_\phi = 0 \tag{5-18c}$$

Using (3-15) or (3-10) with $\mathbf{J} = 0$, the corresponding electric field components can be written as

$$\boxed{E_r = E_\theta = 0} \tag{5-19a}$$

$$\boxed{E_\phi = \eta \frac{(ka)^2 I_0 \sin\theta}{4r}\left[1 + \frac{1}{jkr}\right] e^{-jkr}} \tag{5-19b}$$

5.2.2 Small Loop and Infinitesimal Magnetic Dipole

A comparison of (5-18a)–(5-19b) with those of the infinitesimal magnetic dipole indicates that they have similar forms. In fact, the electric and magnetic field components of an infinitesimal magnetic dipole of length l and constant "magnetic" current I_m are given by

$$E_r = E_\theta = H_\phi = 0 \tag{5-20a}$$

$$E_\phi = -j\frac{kI_m l \sin\theta}{4\pi r}\left[1 + \frac{1}{jkr}\right] e^{-jkr} \tag{5-20b}$$

$$H_r = \frac{I_m l \cos\theta}{2\pi\eta r^2}\left[1 + \frac{1}{jkr}\right] e^{-jkr} \tag{5-20c}$$

$$H_\theta = j\frac{kI_m l \sin\theta}{4\pi\eta r}\left[1 + \frac{1}{jkr} - \frac{1}{(kr)^2}\right] e^{-jkr} \tag{5-20d}$$

These can be obtained from the fields of an infinitesimal electric dipole, (4-8a)–(4-10c). When (5-20a)–(5-20d) are compared with (5-18a)–(5-19b), they indicate that *a magnetic dipole of magnetic moment $I_m l$ is equivalent to a small electric loop of radius a and constant electric current I_0 provided that*

$$\boxed{I_m l = jS\omega\mu I_0} \tag{5-21}$$

where $S = \pi a^2$ (area of the loop). Thus, for analysis purposes, the small electric loop can be replaced by a small linear magnetic dipole of constant current. The geometrical equivalence is illustrated in Figure 5.1(a) where the magnetic dipole is directed along the z-axis which is also perpendicular to the plane of the loop.

5.2.3 Power Density and Radiation Resistance

The fields radiated by a small loop, as given by (5-18a)–(5-19b), are valid everywhere except at the origin. As was discussed in Section 4.1 for the infinitesimal dipole, the power in the region very close to the antenna (near-field, $kr \ll 1$) is predominantly reactive and in the far-field ($kr \gg 1$) is predominantly real. To illustrate this for the loop, the complex power density

$$\begin{aligned}\mathbf{W} &= \tfrac{1}{2}(\mathbf{E} \times \mathbf{H}^*) = \tfrac{1}{2}[(\hat{\mathbf{a}}_\phi E_\phi) \times (\hat{\mathbf{a}}_r H^*_r + \hat{\mathbf{a}}_\theta H^*_\theta)] \\ &= \tfrac{1}{2}(-\hat{\mathbf{a}}_r E_\phi H^*_\theta + \hat{\mathbf{a}}_\theta E_\phi H^*_r)\end{aligned} \tag{5-22}$$

is first formed. When (5-22) is integrated over a closed sphere, only its radial component given by

$$W_r = \eta \frac{(ka)^4}{32} |I_0|^2 \frac{\sin^2 \theta}{r^2} \left[1 + j \frac{1}{(kr)^3} \right] \tag{5-22a}$$

contributes to the complex power P_r. Thus

$$P_r = \oiint_S \mathbf{W} \cdot d\mathbf{s} = \eta \frac{(ka)^4}{32} |I_0|^2 \int_0^{2\pi} \int_0^{\pi} \left[1 + j \frac{1}{(kr)^3} \right] \sin^3 \theta \, d\theta \, d\phi \tag{5-23}$$

which reduces to

$$P_r = \eta \left(\frac{\pi}{12} \right) (ka)^4 |I_0|^2 \left[1 + j \frac{1}{(kr)^3} \right] \tag{5-23a}$$

and whose real part is equal to

$$P_{\text{rad}} = \eta \left(\frac{\pi}{12} \right) (ka)^4 |I_0|^2 \tag{5-23b}$$

For small values of kr ($kr \ll 1$), the second term within the brackets of (5-23a) is dominant which makes the power mainly reactive. In the far-field ($kr \gg 1$), the second term within the brackets diminishes which makes the power real. A comparison between (5-23a) with (4-14) indicates a difference in sign between the terms within the brackets. Whereas for the infinitesimal dipole the radial power density in the near-field is capacitive, for the small loop it is inductive. This indicates that the radial magnetic energy is larger than the electric energy.

The radiation resistance of the loop is found by equating (5-23b) to $|I_0|^2 R_r/2$. Doing this, the radiation resistance can be written as

$$\boxed{R_r = \eta \left(\frac{\pi}{6} \right) (k^2 a^2)^2 = \eta \frac{2\pi}{3} \left(\frac{kS}{\lambda} \right)^2 = 20\pi^2 \left(\frac{C}{\lambda} \right)^4 = 31.171 \left(\frac{S^2}{\lambda^4} \right)} \tag{5-24}$$

where $S = \pi a^2$ is the area and $C = 2\pi a$ is the circumference of the loop.

The radiation resistance as given by (5-24) is only for a single-turn loop. If the loop antenna has N turns wound so that the magnetic field passes through all the loops, the radiation resistance is equal to that of single turn multiplied by N^2. That is,

$$\boxed{R_r = \eta \left(\frac{2\pi}{3} \right) \left(\frac{kS}{\lambda} \right)^2 N^2 = 20\pi^2 \left(\frac{C}{\lambda} \right)^4 N^2 = 31.171 \, N^2 \left(\frac{S^2}{\lambda^4} \right)} \tag{5-24a}$$

Even though the radiation resistance of a single turn loop may be small, the overall value can be increased by including many turns. This is a very desirable and practical mechanism that is not available for the infinitesimal dipole.

Example 5.1

Find the radiation resistance of a single-turn and an 8-turn small circular loop. The radius of the loop is $\lambda/25$ and the medium is free-space.

SOLUTION

$$S = \pi a^2 = \pi\left(\frac{\lambda}{25}\right)^2 = \frac{\pi\lambda^2}{625}$$

$$R_r \text{ (single turn)} = 120\pi\left(\frac{2\pi}{3}\right)\left(\frac{2\pi^2}{625}\right)^2 = 0.788 \text{ ohms}$$

$$R_r \text{ (8 turns)} = 0.788(8)^2 = 50.43 \text{ ohms}$$

The radiation and loss resistances of an antenna determine the radiation efficiency, as defined by (2-90). The loss resistance of a single-turn small loop is, in general, much larger than its radiation resistance; thus the corresponding radiation efficiencies are very low and depend on the loss resistance. To increase the radiation efficiency, multiturn loops are often employed. However, because the current distribution in a multiturn loop is quite complex, great confidence has not yet been placed in analytical methods for determining the radiation efficiency. Therefore greater reliance has been placed on experimental procedures. Two experimental techniques that can be used to measure the radiation efficiency of a small multiturn loop are those that are usually referred to as the *Wheeler method* and the *Q method* [1].

Usually it is assumed that the loss resistance of a small loop is the same as that of a straight wire whose length is equal to the circumference of the loop, and it is computed using (2-90b). Although this assumption is adequate for single-turn loops, it is not valid for multiturn loops. In a multiturn loop, the current is not uniformly distributed around the wire but depends on the skin and proximity effects [2]. In fact, for close spacings between turns, the contribution to the loss resistance due to the proximity effect can be larger than that due to the skin effect.

The total ohmic resistance for an N-turn circular loop antenna with loop radius a, wire radius b, and loop separation $2c$, shown in Figure 5.2(a) is given by [3]

$$R_{\text{ohmic}} = \frac{Na}{b}R_s\left(\frac{R_p}{R_0} + 1\right) \tag{5-25}$$

where

$$R_s = \sqrt{\frac{\omega\mu_0}{2\sigma}} = \text{surface impedance of conductor}$$

$$R_p = \text{ohmic resistance per unit length due to proximity effect}$$

$$R_0 = \frac{NR_s}{2\pi b} = \text{ohmic skin effect resistance per unit length (ohms/m)}$$

The ratio of R_p/R_0 has been computed [3] as a function of the spacing c/b for loops with $2 \leq N \leq 8$ and it is shown plotted in Figure 5.2(b). It is evident that for close spacing the ohmic resistance is twice as large as that in the absence of the proximity effect ($R_p/R_0 = 0$).

Example 5.2

Find the radiation efficiency of a single-turn and an 8-turn small circular loop at $f = 100$ MHz. The radius of the loop is $\lambda/25$, the radius of the wire is $10^{-4}\lambda$, and

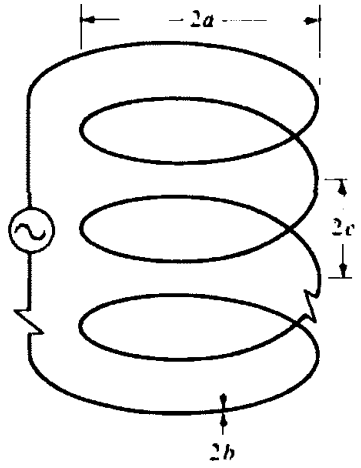

(a) N-turn circular loop

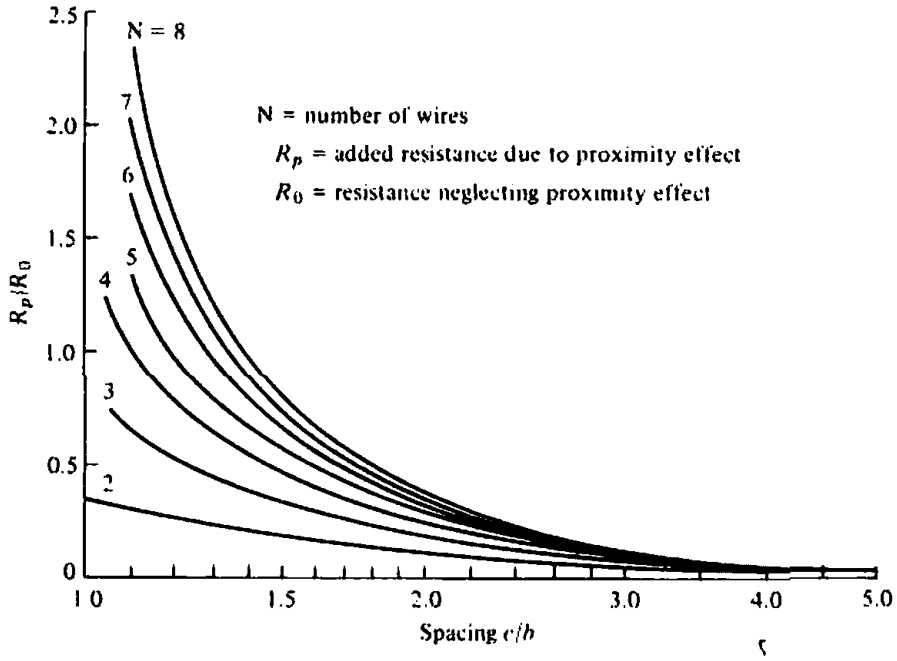

(b) Ohmic resistance due to proximity (after G. N. Smith)

Figure 5.2 N-turn circular loop and ohmic resistance due to proximity effect. (SOURCE: G. S. Smith, "Radiation Efficiency of Electrically Small Multiturn Loop Antennas," *IEEE Trans. Antennas Propagat.*, Vol. AP-20, No. 5, pp. 656-657, Sept. 1972© (1972) IEEE).

the turns are spaced $4 \times 10^{-4}\lambda$ apart. Assume the wire is copper with a conductivity of 5.7×10^7 (S/m) and the antenna is radiating into free-space.

SOLUTION

From Example 5.1

$$R_r \text{ (single turn)} = 0.788 \text{ ohms}$$

$$R_r \text{ (8 turns)} = 50.43 \text{ ohms}$$

The loss resistance for a single turn is given, according to (2-90b), by

$$R_L = R_{hf} = \frac{a}{b}\sqrt{\frac{\omega\mu_0}{2\sigma}} = \frac{1}{25(10^{-4})}\sqrt{\frac{\pi(10^8)(4\pi \times 10^{-7})}{5.7 \times 10^7}}$$
$$= 1.053 \text{ ohms}$$

and the radiation efficiency, according to (2-90), by

$$e_{cd} = \frac{0.788}{0.788 + 1.053} = 0.428 = 42.8\%$$

From Figure 5.2(*b*)

$$\frac{R_R}{R_0} = 0.38$$

and from (5-25)

$$R_L = R_{\text{ohmic}} = \frac{8}{25(10^{-4})}\sqrt{\frac{\pi(10^8)(4\pi \times 10^{-7})}{5.7 \times 10^7}}(1.38) = 11.62$$

Thus

$$e_{cd} = \frac{50.43}{50.43 + 11.62} = 0.813 = 81.3\%$$

5.2.4 Near-Field ($kr \ll 1$) Region

The expressions for the fields, as given by (5-18a)–(5-19b), can be simplified if the observations are made in the near-field ($kr \ll 1$). As for the infinitesimal dipole, the predominant term in each expression for the field in the near-zone region is the last one within the parentheses of (5-18a)–(5-19b). Thus for $kr \ll 1$

$$H_r \simeq \frac{a^2 I_0 e^{-jkr}}{2r^3}\cos\theta \qquad \text{(5-26a)}$$

$$H_\theta \simeq \frac{a^2 I_0 e^{-jkr}}{4r^3}\sin\theta \qquad \text{(5-26b)}$$

$$H_\phi = E_r = E_\theta = 0 \qquad \text{(5-26c)}$$

$$E_\phi \simeq -j\frac{a^2 k I_0 e^{-jkr}}{4r^2}\sin\theta \qquad \text{(5-26d)}$$

$kr \ll 1$

The two **H**-field components are in time-phase. However, they are in time quadrature with those of the electric field. This indicates that the average power (real power) is zero, as for the infinitesimal electric dipole. The condition of $kr \ll 1$ can be satisfied at moderate distances away from the antenna provided the frequency of operation is very low. The fields of (5-26a)–(5-26d) are usually referred to as *quasi-stationary*.

5.2.5 Far-Field ($kr \gg 1$) Region

The other space of interest where the fields can be approximated is the far-field ($kr \gg 1$) region. In contrast to the near-field, the dominant term in (5-18a)–(5-19b) for $kr \gg 1$ is the first one within the parentheses. Since for $kr > 1$ the H_r component will be inversely proportional to r^2 whereas H_θ will be inversely proportional to r, for large values of kr ($kr \gg 1$) the H_r component will be small compared to H_θ. Thus it can be assumed that it is approximately equal to zero. Therefore for $kr \gg 1$,

$$\left.\begin{aligned} H_\theta &\simeq -\frac{k^2a^2I_0e^{-jkr}}{4r}\sin\theta = -\frac{\pi SI_0e^{-jkr}}{\lambda^2 r}\sin\theta \\ E_\phi &\simeq \eta\frac{k^2a^2I_0e^{-jkr}}{4r}\sin\theta = \eta\frac{\pi SI_0e^{-jkr}}{\lambda^2 r}\sin\theta \end{aligned}\right\} \quad kr \gg 1 \qquad \begin{matrix}(5\text{-}27a)\\(5\text{-}27b)\end{matrix}$$

$$H_r \simeq H_\phi = E_r = E_\theta = 0 \qquad (5\text{-}27c)$$

where $S = \pi a^2$ is the geometrical area of the loop.

Forming the ratio of $-E_\phi/H_\theta$, the wave impedance can be written as

$$Z_w = -\frac{E_\phi}{H_\theta} \simeq \eta \qquad (5\text{-}28)$$

where

Z_w = wave impedance
η = intrinsic impedance

As for the infinitesimal dipole, the **E**- and **H**-field components of the loop in the far-field ($kr \gg 1$) region are perpendicular to each other and transverse to the direction of propagation. They form a *T*ransverse *E*lectro *M*agnetic (TEM) field whose wave impedance is equal to the intrinsic impedance of the medium. Equations (5-27a)–(5-27c) can also be derived using the procedure outlined and relationships developed in Section 3.6. This is left as an exercise to the reader (Prob. 5.5).

5.2.6 Radiation Intensity and Directivity

The real power P_{rad} radiated by the loop was found in Section 5.2.3 and is given by (5-23b). The same expression can be obtained by forming the average power density, using (5-27a)–(5-27c), and integrating it over a closed sphere of radius r. This is left as an exercise to the reader (Prob. 5.4). Associated with the radiated power P_{rad} is an average power density $\mathbf{W}_{av}$. It has only a radial component W_r which is related to the radiation intensity U by

$$U = r^2W_r = \frac{\eta}{2}\left(\frac{k^2a^2}{4}\right)^2|I_0|^2\sin^2\theta = \frac{r^2}{2\eta}|E_\phi(r,\theta,\phi)|^2 \qquad (5\text{-}29)$$

and it conforms to (2-12a). The normalized pattern of the loop, as given by (5-29), is identical to that of the infinitesimal dipole shown in Figure 4.2. The maximum value occurs at $\theta = \pi/2$, and it is given by

$$U_{max} = U|_{\theta=\pi/2} = \frac{\eta}{2}\left(\frac{k^2a^2}{4}\right)^2|I_0|^2 \qquad (5\text{-}30)$$

Using (5-30) and (5-23b), the directivity of the loop can be written as

$$\boxed{D_0 = 4\pi \frac{U_{\max}}{P_{\text{rad}}} = \frac{3}{2}} \tag{5-31}$$

and its maximum effective aperture as

$$\boxed{A_{em} = \left(\frac{\lambda^2}{4\pi}\right) D_0 = \frac{3\lambda^2}{8\pi}} \tag{5-32}$$

It is observed that the directivity, and as a result the maximum effective area, of a small loop is the same as that of an infinitesimal electric dipole. This should be expected since their patterns are identical.

The far-field expressions for a small loop, as given by (5-27a)–(5-27c), will be obtained by another procedure in the next section. In that section a loop of any radius but of constant current will be analyzed. Closed form solutions will be possible only in the far-field region. The small loop far-field expressions will then be obtained as a special case of that problem.

Example 5.3

The radius of a small loop of constant current is $\lambda/25$. Find the physical area of the loop and compare it with its maximum effective aperture.

SOLUTION

$$S \text{ (physical)} = \pi a^2 = \pi\left(\frac{\lambda}{25}\right)^2 = \frac{\pi\lambda^2}{625} = 5.03 \times 10^{-3}\lambda^2$$

$$A_{em} = \frac{3\lambda^2}{8\pi} = 0.119\lambda^2$$

$$\frac{A_{em}}{S} = \frac{0.119\lambda^2}{5.03 \times 10^{-3}\lambda^2} = 23.66$$

Electrically the loop is about 24 times larger than its physical size, which should not be surprising. To be effective, a small loop must be larger electrically than its physical size.

5.2.7 Equivalent Circuit

A small loop is primarily inductive, and it can be represented by a lumped element equivalent circuit similar to those of Figure 2.22.

A. Transmitting Mode

The equivalent circuit for its input impedance when the loop is used as a transmitting antenna is that shown in Figure 5.3. This is similar to the equivalent circuit of Figure 2.22(b). Therefore its input impedance Z_{in} is represented by

$$Z_{in} = R_{in} + jX_{in} = (R_r + R_L) + j(X_A + X_i) \tag{5-33}$$

where

R_r = radiation resistance as given by (5-24)
R_L = loss resistance of loop conductor
X_A = external inductive reactance of loop antenna = ωL_A
X_i = internal high-frequency reactance of loop conductor = ωL_i

In Figure 5.3 the capacitor C_r is used in parallel to (5-33) to resonate the antenna; it can also be used to represent distributed stray capacitances. In order to determine the capacitance of C_r at resonance, it is easier to represent (5-33) by its equivalent admittance Y_{in} of

$$Y_{in} = G_{in} + jB_{in} = \frac{1}{Z_{in}} = \frac{1}{R_{in} + jX_{in}} \tag{5-34}$$

where

$$G_{in} = \frac{R_{in}}{R_{in}^2 + X_{in}^2} \tag{5-34a}$$

$$B_{in} = -\frac{X_{in}}{R_{in}^2 + X_{in}^2} \tag{5-34b}$$

At resonance, the susceptance B_r of the capacitor C_r must be chosen to eliminate the imaginary part B_{in} of (5-34) and (5-34a). This is accomplished by choosing C_r according to

$$C_r = \frac{B_r}{2\pi f} = -\frac{B_{in}}{2\pi f} = \frac{1}{2\pi f}\frac{X_{in}}{R_{in}^2 + X_{in}^2} \tag{5-35}$$

Under resonance the input impedance Z'_{in} is then equal to

$$Z'_{in} = R'_{in} = \frac{1}{G_{in}} = \frac{R_{in}^2 + X_{in}^2}{R_{in}} = R_{in} + \frac{X_{in}^2}{R_{in}} \tag{5-36}$$

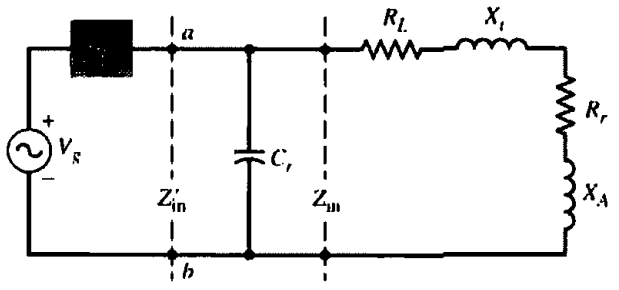

Figure 5.3 Equivalent circuit of loop antenna in transmitting mode.

The loss resistance R_L of the loop conductor can be computed using techniques illustrated in Example 5.2. The inductive reactance X_A of the loop is computed using the inductance L_A of:

Circular loop of radius a and wire radius b:

$$L_A = \mu_0 a\left[\ln\left(\frac{8a}{b}\right) - 2\right] \tag{5-37a}$$

Square loop with sides a and wire radius b:

$$L_A = 2\mu_0\frac{a}{\pi}\left[\ln\left(\frac{a}{b}\right) - 0.774\right] \tag{5-37b}$$

The internal reactance of the loop conductor X_i can be found using the internal inductance L_i of the loop which for a single turn can be approximated by

$$L_i = \frac{l}{\omega P}\sqrt{\frac{\omega\mu_0}{2\sigma}} = \frac{a}{\omega b}\sqrt{\frac{\omega\mu_0}{2\sigma}} \tag{5-38}$$

where l is the length and P is the perimeter of the wire of the loop

B. Receiving Mode

The loop antenna is often used as a receiving antenna or as a probe to measure magnetic flux density. Therefore when a plane wave impinges upon it, as shown in Figure 5.4(a), an open-circuit voltage develops across its terminals. This open-circuit voltage is related according to (2-93) to its vector effective length and incident electric field. This open-circuit voltage is proportional to the incident magnetic flux density B_z^i, which is normal to the plane of the loop. Assuming the incident field is uniform over the plane of the loop, the open-circuit voltage for a single-turn loop can be written as [5]

$$V_{oc} = j\omega\pi a^2 B_z^i \tag{5-39}$$

Defining in Figure 5.4(a) the plane of incidence as the plane formed by the z axis and radical vector, then the open-circuit voltage of (5-39) can be related to the magnitude of the incident magnetic and electric fields by

$$V_{oc} = j\omega\pi a^2\mu_0 H^i \cos\psi_i \sin\theta_i = jk_0\pi a^2 E^i \cos\psi_i \sin\theta_i \tag{5-39a}$$

where ψ_i is the angle between the direction of the magnetic field of the incident plane wave and the plane of incidence, as shown in Figure 5.4(a).

Since the open-circuit voltage is also related to the vector effective length by (2-93), then the effective length for a single turn loop can be written as

$$\ell_e = \hat{\mathbf{a}}_\phi l_e = \hat{\mathbf{a}}_\phi jk_0\pi a^2 \cos\psi_i \sin\theta_i = \hat{\mathbf{a}}_\phi jk_0 S\cos\psi_i \sin\theta_i \tag{5-40}$$

where S is the area of the loop. The factor $\cos\psi_i \sin\theta_i$ is introduced because the open-circuit voltage is proportional to the magnetic flux density component B_z^i which is normal to the plane of the loop.

When a load impedance Z_L is connected to the output terminals of the loop as shown in Figure 5.4(b), the voltage V_L across the load impedance Z_L is related to the input impedance Z_{in}' of Figure 5.4(b) and the open-circuit voltage of (5-39a) by

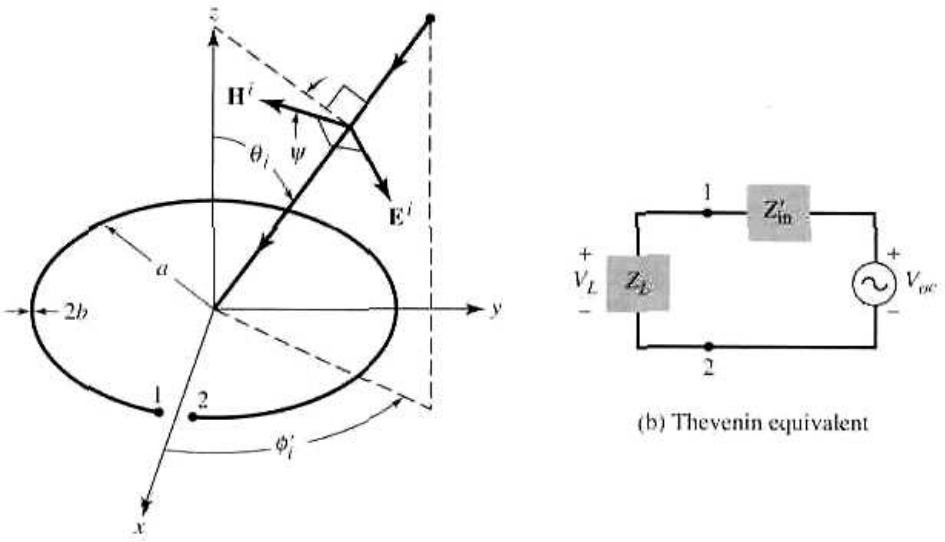

(b) Thevenin equivalent

(a) Plane wave incident on a receiving loop (G.S. Smith, "Loop Antennas," Copyright © 1984, McGraw-Hill, Inc. Permission by McGraw-Hill, Inc.)

Figure 5.4 Loop antenna and its equivalent in receiving mode.

$$V_L = V_{oc} \frac{Z_L}{Z_{\text{in}}' + Z_L} \tag{5-41}$$

5.3 CIRCULAR LOOP OF CONSTANT CURRENT

Let us now reconsider the loop antenna of Figure 5.1(a) but with a radius that may not necessarily be small. The current in the loop will again be assumed to be constant, as given by (5-1). For this current distribution, the vector potential is given by (5-14). Without using the small radius approximation, the integration in (5-14) cannot be carried out. However, if the observations are restricted in the far-field ($r \gg a$) region, the small radius approximation is not needed to integrate (5-14).

Although the uniform current distribution along the perimeter of the loop is only valid provided the circumference is less than about 0.2λ (radius less than about 0.03λ), the procedure developed here for a constant current can be followed to find the far zone fields of any size loop with not necessarily uniform current.

5.3.1 Radiated Fields

To find the fields in the far-field region, the distance R can be approximated by

$$R = \sqrt{r^2 + a^2 - 2ar \sin\theta \cos\phi'} \simeq \sqrt{r^2 - 2ar \sin\theta \cos\phi'} \qquad \text{for} \quad r \gg a \tag{5-42}$$

which can be reduced, using the binomial expansion, to

$$\left.\begin{aligned} R &\simeq r\sqrt{1 - \frac{2a}{r}\sin\theta\cos\phi'} = r - a\sin\theta\cos\phi' = r - a\cos\psi_0 \qquad \text{for phase terms} \\ R &\simeq r \qquad\qquad\qquad\qquad\qquad\qquad\qquad\qquad\qquad\quad \text{for amplitude terms} \end{aligned}\right\} \tag{5-43}$$

since

$$\begin{aligned}\cos\psi_0 &= \hat{\mathbf{a}}_\rho' \cdot \hat{\mathbf{a}}_r \,|_{\phi=0} = (\hat{\mathbf{a}}_x \cos\phi' + \hat{\mathbf{a}}_y \sin\phi') \\ &\quad \cdot (\hat{\mathbf{a}}_x \sin\theta\cos\phi + \hat{\mathbf{a}}_y \sin\theta\sin\phi + \hat{\mathbf{a}}_z \cos\theta)|_{\phi=0} \\ &= \sin\theta\cos\phi' \end{aligned} \tag{5-43a}$$

The geometrical relation between R and r, for any observation angle ϕ in the far-field region, is shown in Figure 5.1(b). For observations at $\phi = 0$, it simplifies to that given by (5-43) and shown in Figure 5.5. Thus (5-14) can be written as

$$A_\phi \simeq \frac{a\mu I_0 e^{-jkr}}{4\pi r}\int_0^{2\pi} \cos\phi' e^{+jka\sin\theta\cos\phi'}\, d\phi' \tag{5-44}$$

and it can be separated into two terms as

$$A_\phi \simeq \frac{a\mu I_0 e^{-jkr}}{4\pi r}\left[\int_0^{\pi} \cos\phi' e^{+jka\sin\theta\cos\phi'}\, d\phi' + \int_{\pi}^{2\pi} \cos\phi' e^{+jka\sin\theta\cos\phi'}\, d\phi'\right] \tag{5-45}$$

The second term within the brackets can be rewritten by making a change of variable of the form

$$\phi' = \phi'' + \pi \tag{5-46}$$

Thus (5-45) can also be written as

$$A_\phi \simeq \frac{a\mu I_0 e^{-jkr}}{4\pi r}\left[\int_0^{\pi} \cos\phi' e^{+jka\sin\theta\cos\phi'}\, d\phi' - \int_0^{\pi} \cos\phi'' e^{-jka\sin\theta\cos\phi''}\, d\phi''\right] \tag{5-47}$$

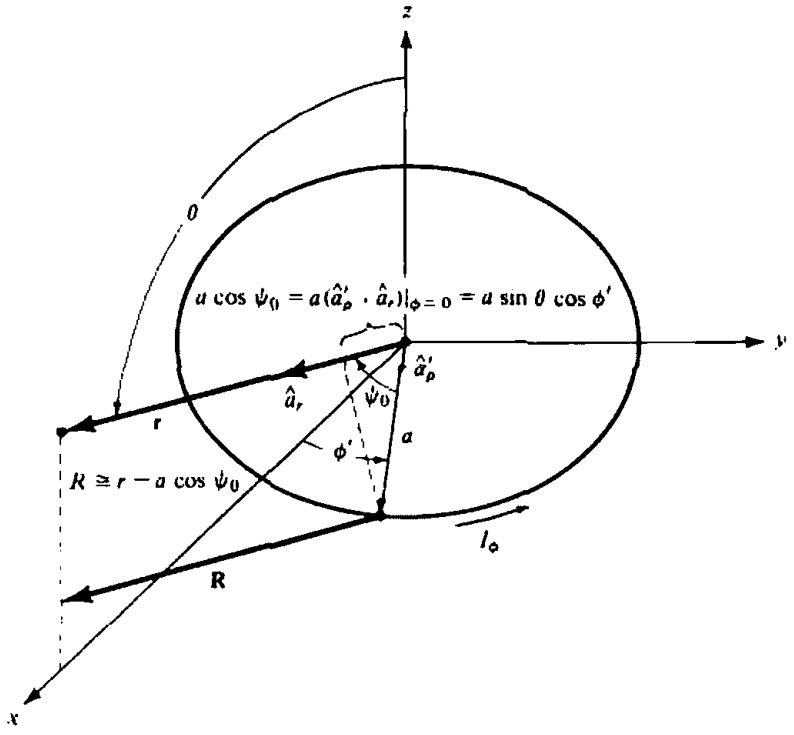

Figure 5.5 Geometry for far-field analysis of a loop antenna.

Each of the integrals in (5-47) can be integrated by the formula (see Appendix V)

$$\pi j^n J_n(z) = \int_0^{\pi} \cos(n\phi) e^{+jz\cos\phi}\, d\phi \tag{5-48}$$

where $J_n(z)$ is the Bessel function of the first kind of order n. Using (5-48) reduces (5-47) to

$$A_\phi \simeq \frac{a\mu I_0 e^{-jkr}}{4\pi r} |\pi j J_1(ka \sin\theta) - \pi j J_1(-ka \sin\theta)| \tag{5-49}$$

The Bessel function of the first kind and order n is defined (see Appendix V) by the infinite series

$$J_n(z) = \sum_{m=0}^{\infty} \frac{(-1)^m (z/2)^{n+2m}}{m!(m+n)!} \tag{5-50}$$

By a simple substitution into (5-50), it can be shown that

$$J_n(-z) = (-1)^n J_n(z) \tag{5-51}$$

which for $n = 1$ is equal to

$$J_1(-z) = -J_1(z) \tag{5-52}$$

Using (5-52) we can write (5-49) as

$$A_\phi \simeq j \frac{a\mu I_0 e^{-jkr}}{2r} J_1(ka \sin\theta) \tag{5-53}$$

The next step is to find the **E**- and **H**-fields associated with the vector potential of (5-53). Since (5-53) is only valid for far-field observations, the procedure outlined in Section 3.6 can be used. The vector potential **A**, as given by (5-53), is of the form suggested by (3-56). That is, the r variations are separable from those of θ and ϕ. Therefore according to (3-58a)–(3-58b) and (5-53)

$$E_r \simeq E_\theta = 0 \tag{5-54a}$$

$$E_\phi \simeq \frac{ak\eta I_0 e^{-jkr}}{2r} J_1(ka \sin\theta) \tag{5-54b}$$

$$H_r \simeq H_\phi = 0 \tag{5-54c}$$

$$H_\theta \simeq -\frac{E_\phi}{\eta} = -\frac{akI_0 e^{-jkr}}{2r} J_1(ka \sin\theta) \tag{5-54d}$$

5.3.2 Power Density, Radiation Intensity, Radiation Resistance, and Directivity

The next objective for this problem will be to find the power density, radiation intensity, radiation resistance, and directivity. To do this, the time-average power density is formed. That is,

$$\mathbf{W}_{av} = \frac{1}{2}\text{Re}[\mathbf{E} \times \mathbf{H}^*] = \frac{1}{2}\text{Re}[\hat{\mathbf{a}}_\phi E_\phi \times \hat{\mathbf{a}}_\theta H^*_\theta] = \hat{\mathbf{a}}_r \frac{1}{2\eta} |E_\phi|^2 \tag{5-55}$$

which can be written using (5-54b) as

$$\mathbf{W}_{av} = \hat{\mathbf{a}}_r W_r = \hat{\mathbf{a}}_r \frac{(a\omega\mu)^2|I_0|^2}{8\eta r^2} J_1^2(ka \sin\theta) \tag{5-56}$$

with the radiation intensity given by

$$U = r^2 W_r = \frac{(a\omega\mu)^2|I_0|^2}{8\eta} J_1^2(ka \sin\theta) \tag{5-57}$$

The radiation patterns for $a = \lambda/10$, $\lambda/5$, and $\lambda/2$ are shown in Figure 5.6. These patterns indicate that the field radiated by the loop along its axis ($\theta = 0°$) is zero. Also the shape of these patterns is similar to that of a linear dipole with $l \leq \lambda$ (a

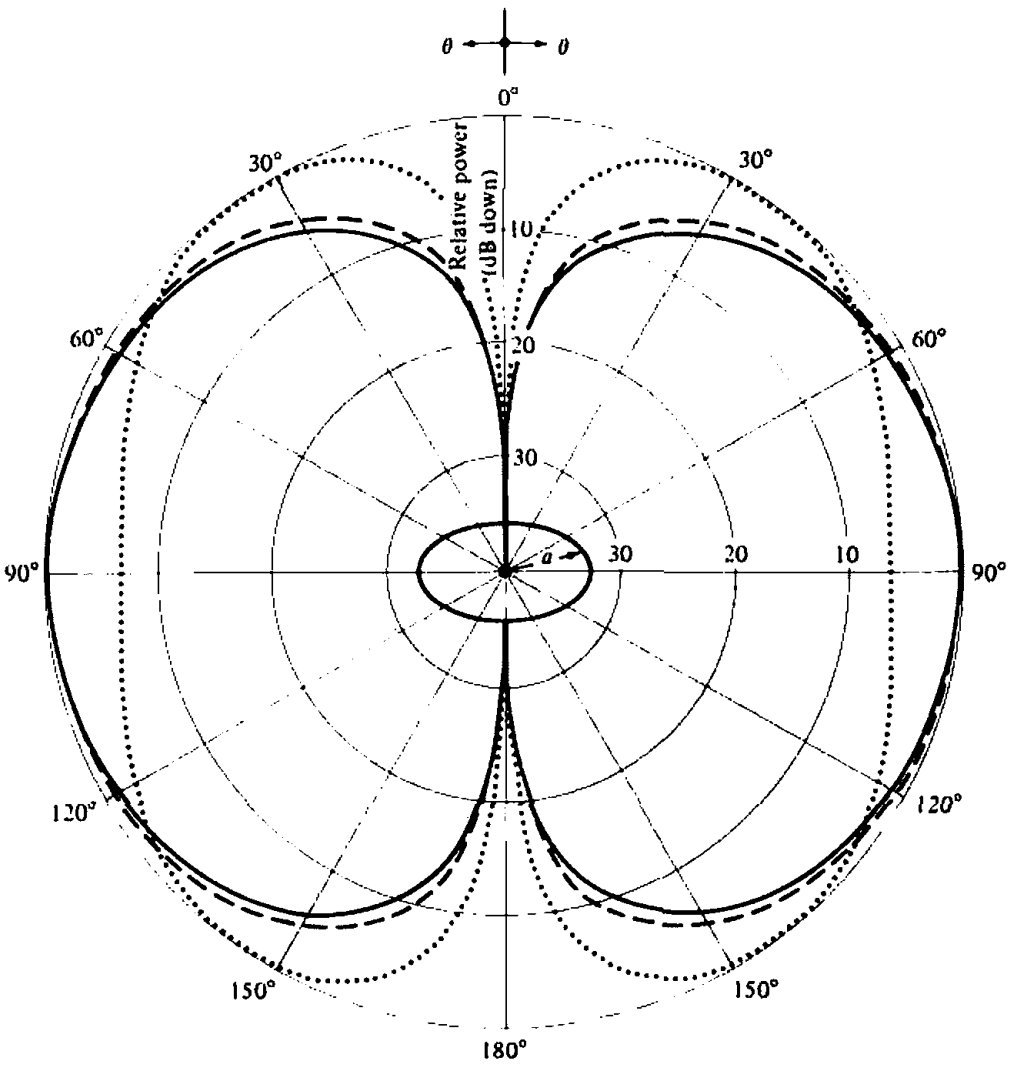

Figure 5.6 Elevation plane amplitude patterns for a circular loop of constant current ($a = 0.1\lambda$, 0.2λ, and 0.5λ).

figure-eight shape). As the radius a increases beyond 0.5λ, the field intensity along the plane of the loop ($\theta = 90°$) diminishes and eventually it forms a null when $a \simeq 0.61\lambda$. This is left as an exercise to the reader for verification (Prob. 5.13). Beyond $a = 0.61\lambda$, the radiation along the plane of the loop begins to intensify and the pattern attains a multilobe form.

The patterns represented by (5-57) (some of them are illustrated in Figure 5.6) assume that the current distribution, no matter what the loop size, is constant. This is not a valid assumption if the loop circumference C ($C = 2\pi a$) exceeds about 0.2λ (i.e., $a > 0.032\lambda$) [6]. For radii much greater than about 0.032λ, the current variation along the circumference of the loop begins to attain a distribution that is best represented by a Fourier series [5]. Although a most common assumption is that the current distribution is nearly cosinusoidal, it is not satisfactory particulary near the driving point of the antenna.

It has been shown [7] that when the circumference of the loop is about one wavelength ($C \simeq \lambda$), its maximum radiation is along its axis ($\theta = 0°$) which is perpendicular to the plane of the loop. This feature of the loop antenna has been utilized to design Yagi-Uda arrays whose basic elements (feed, directors, and reflectors) are circular loops [8]–[10]. Because of its many applications, the one wavelength circumference circular loop antenna is considered as fundamental as a half-wavelength dipole.

The radiated power can be written using (5-56) as

$$P_{\text{rad}} = \iint_S \mathbf{W}_{\text{av}} \cdot d\mathbf{s} = \frac{\pi(a\omega\mu)^2|I_0|^2}{4\eta} \int_0^{\pi} J_1^2(ka \sin\theta) \sin\theta \, d\theta \tag{5-58}$$

The integral in (5-58) cannot be integrated exactly. However, it can be rewritten [11] as

$$\int_0^{\pi} J_1^2(ka \sin\theta) \sin\theta \, d\theta = \frac{1}{ka} \int_0^{2ka} J_2(x) \, dx \tag{5-59}$$

Even though (5-59) still cannot be integrated, approximations can be made depending upon the values of the upper limit (the radius of the loop).

A. Large Loop Approximation ($a \geq \lambda/2$)

To evaluate (5-59), the first approximation will be to assume that the radius of the loop is large ($a \geq \lambda/2$). For that case, the integral in (5-59) can be approximated by

$$\int_0^{\pi} J_1^2(ka \sin\theta) \sin\theta \, d\theta = \frac{1}{ka} \int_0^{2ka} J_2(x) \, dx \simeq \frac{1}{ka} \tag{5-60}$$

and (5-58) by

$$P_{\text{rad}} \simeq \frac{\pi(a\omega\mu)^2|I_0|^2}{4\eta(ka)} \tag{5-61}$$

The maximum radiation intensity occurs when $ka \sin\theta = 1.84$ so that

$$U|_{\max} = \frac{(a\omega\mu)^2|I_0|^2}{8\eta} J_1^2(ka \sin\theta)|_{ka\sin\theta = 1.84} = \frac{(a\omega\mu)^2|I_0|^2}{8\eta}(0.584)^2 \tag{5-62}$$

Thus

$$R_r = \frac{2P_{\text{rad}}}{|I_0|^2} = \frac{2\pi(a\omega\mu)^2}{4\eta(ka)} = \eta\left(\frac{\pi}{2}\right)ka = 60\pi^2(ka) = 60\pi^2\left(\frac{C}{\lambda}\right) \quad (5\text{-}63a)$$

$$D_0 = 4\pi\frac{U_{\max}}{P_{\text{rad}}} = 4\pi\frac{ka(0.584)^2}{2\pi} = 2ka(0.584)^2 = 0.682\left(\frac{C}{\lambda}\right) \quad (5\text{-}63b)$$

$$A_{em} = \frac{\lambda^2}{4\pi}D_0 = \frac{\lambda^2}{4\pi}\left[0.682\left(\frac{C}{\lambda}\right)\right] = 5.43 \times 10^{-2}\lambda C \quad (5\text{-}63c)$$

where C (circumference) $= 2\pi a$ and $\eta \simeq 120\pi$.

B. Intermediate Loop Approximation ($\lambda/6\pi \leq a < \lambda/2$)
If the radius of the loop is $\lambda/6\pi \leq a < \lambda/2$, the integral of (5-59) can be approximated by

$$\int_0^{\pi} J_1^2(ka\sin\theta)\sin\theta\, d\theta = \frac{1}{ka}\int_0^{2ka} J_2(x)\, dx$$
$$\simeq \frac{1}{ka}\left[-2J_1(2ka) + \int_0^{2ka} J_0(y)\, dy\right] \quad (5\text{-}64)$$

where $J_0(y)$ is the Bessel function of the first kind of zero order. No further simplifications can be made. The integral of $J_0(y)$ appearing in (5-64) is a tabulated function which is included in Appendix V. The radiation resistance, directivity, and maximum effective area can be found using (5-64) to evaluate the P_{rad} of (5-58).

C. Small Loop Approximation ($a < \lambda/6\pi$)
If the radius of the loop is small ($a < \lambda/6\pi$), the expressions for the fields as given by (5-54a)–(5-54d) can be simplified. To do this, the Bessel function $J_1(ka\sin\theta)$ is expanded, by the definition of (5-50), in an infinite series of the form (see Appendix V)

$$J_1(ka\sin\theta) = \tfrac{1}{2}(ka\sin\theta) - \tfrac{1}{16}(ka\sin\theta)^3 + \cdots \quad (5\text{-}65)$$

For small values of ka ($ka < \frac{1}{3}$), (5-65) can be approximated by its first term, or

$$J_1(ka\sin\theta) \simeq \frac{ka\sin\theta}{2} \quad (5\text{-}65a)$$

Thus (5-54a)–(5-54d) can be written as

$$E_r \simeq E_\theta = 0 \quad (5\text{-}66a)$$

$$E_\phi \simeq \frac{a^2\omega\mu k I_0 e^{-jkr}}{4r}\sin\theta = \eta\frac{a^2k^2I_0e^{-jkr}}{4r}\sin\theta \quad (5\text{-}66b)$$

$$H_r \simeq H_\phi = 0 \quad (5\text{-}66c)$$

$$H_\theta \simeq -\frac{a^2\omega\mu k I_0 e^{-jkr}}{4\eta r}\sin\theta = -\frac{a^2k^2I_0e^{-jkr}}{4r}\sin\theta \quad (5\text{-}66d)$$

$$\Big\} \; a < \lambda/6\pi$$

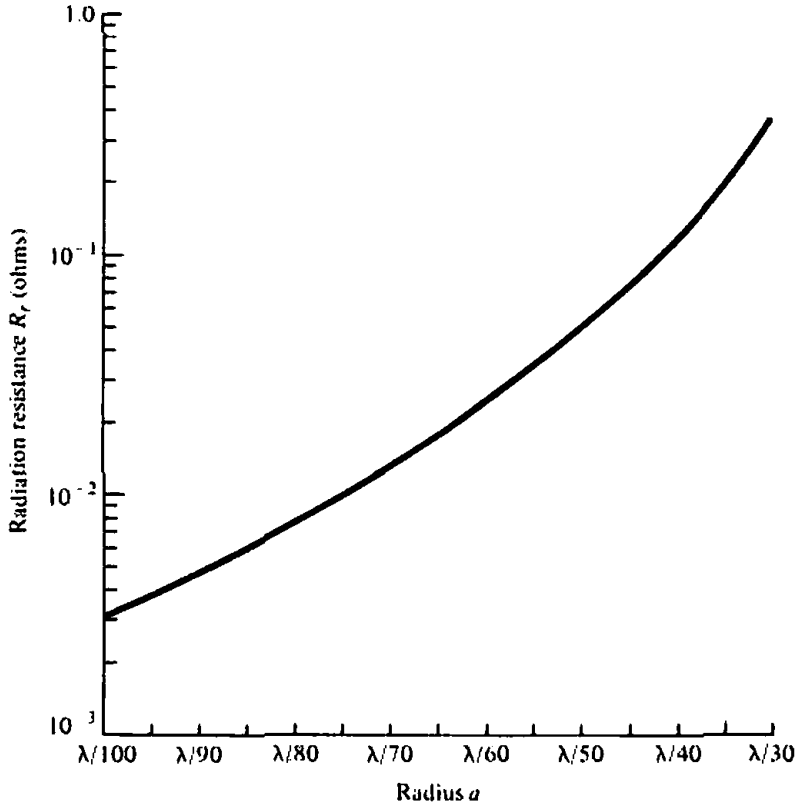

Figure 5.7 Radiation resistance for a constant current circular loop antenna based on the approximation of (5-65a).

which are identical to those of (5-27a)–(5-27c). Thus the expressions for the radiation resistance, radiation intensity, directivity, maximum effective aperture, and radiation resistance are those given by (5-24), (5-29), (5-31), and (5-32).

To demonstrate the variation of the radiation resistance as a function of the radius a of the loop, it is plotted in Figure 5.7 for $\lambda/100 \leq a \leq \lambda/30$, based on the approximation of (5-65a). It is evident that the values are extremely low (less than 1 ohm), and they are usually smaller than the loss resistances of the wires. These radiation resistances also lead to large mismatch losses when connected to practical transmission lines of 50 or 75 ohms. To increase the radiation resistance, it would require multiple turns as suggested by (5-24a). This, however, also increases the loss resistance which contributes to the inefficiency of the antenna. A plot of the radiation resistance for $0 < ka = C/\lambda < 20$, based on the evaluation of (5-59) by numerical techniques, is shown in Figure 5.8. The dashed line represents the values based on the large loop approximation of (5-60) and the dotted ($\cdots\cdots$) represents the values based on the small loop approximation of (5-65a).

In addition to the real part of the input impedance, there is also an imaginary component which would increase the mismatch losses even if the real part is equal to the characteristic impedance of the lossless transmission line. However, the imaginary component can always, in principle at least, be eliminated by connecting a reactive element (capacitive or inductive) across the terminals of the loop to make the antenna a resonant circuit.

To facilitate the computations for the directivity and radiation resistance of a circular loop with a constant current distribution, a FORTRAN computer program has

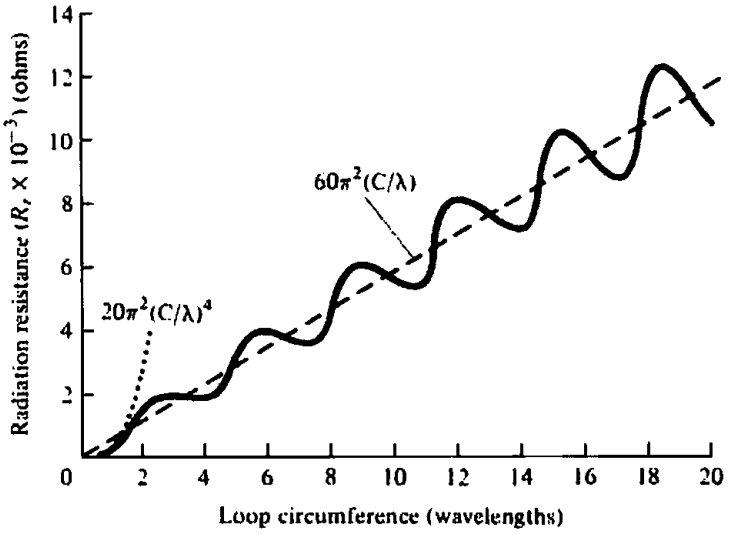

(a) Radiation resistance of circular loop

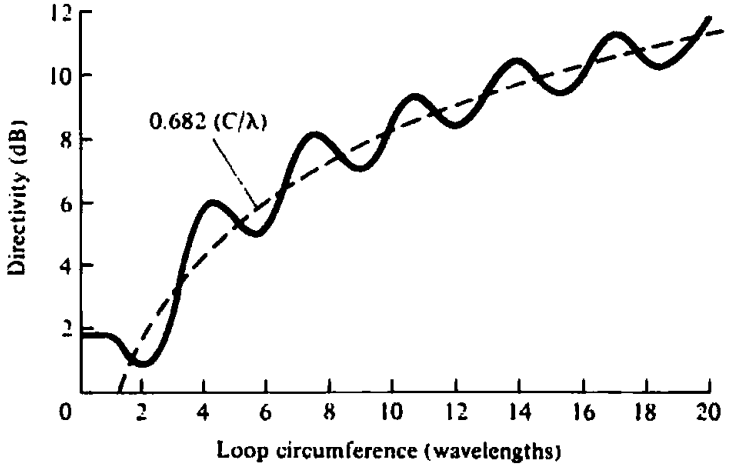

(b) Directivity of circular loop

Figure 5.8 Radiation resistance and directivity for circular loop of constant current. (SOURCE: E. A. Wolff, *Antenna Analysis*, Wiley, New York, 1966)

been developed. The program utilizes (5-62) and (5-58) to compute the directivity [(5-58) is integrated numerically]. The program requires as an input the radius of the loop (in wavelengths). A Bessel function subroutine is contained within the program. A listing of the program is included at the end of this chapter and in the computer disc included with the book.

5.4 CIRCULAR LOOP WITH NONUNIFORM CURRENT

The analysis in the previous sections was based on a uniform current, which would be a valid approximation when the radius of the loop is small electrically (usually $a < 0.03\lambda$). As the dimensions of the loop increase, the current variations along the circumference of the loop must be taken into account. As stated previously, a very common assumption for the current distribution is a cosinusoidal variation [12], [13]. This, however, is not a satisfactory approximation particularly near the driving point

of the antenna [6]. A better distribution would be to represent the current by a Fourier series [14]

$$I(\phi') = I_0 + 2\sum_{n=1}^{M} I_n \cos(n\phi') \tag{5-67}$$

where ϕ' is measured from the feed point of the loop along the circumference, as shown at the inset of Figure 5.9.

A complete analysis of the fields radiated by a loop with nonuniform current distribution is somewhat complex, laborious, and quite lengthy. Instead of attempting to include the analytical formulations, which are cumbersome but well documented in the cited references, a number of graphical illustrations of numerical and experimental data is presented. These curves can be used in facilitating designs.

To illustrate that the current distribution of a wire loop antenna is not uniform unless its radius is very small, the magnitude and phase of it have been plotted in Figure 5.9 as a function of ϕ' (in degrees). The loop circumference C is $ka = C/\lambda$

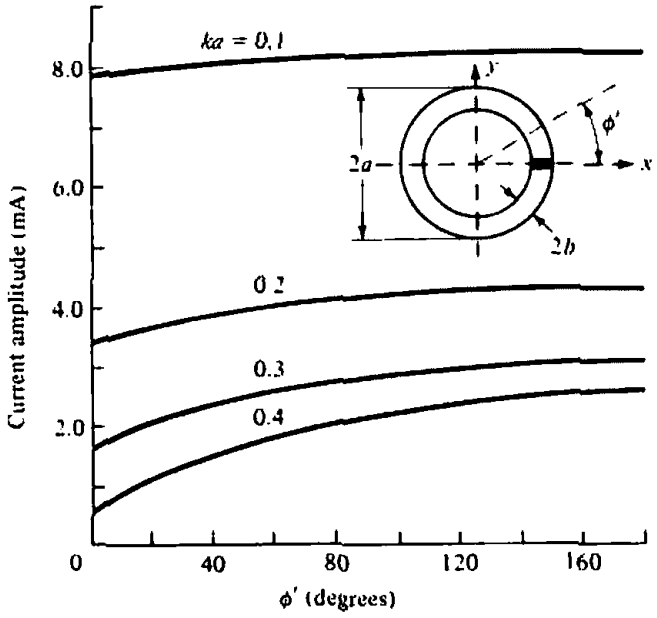

(a) Magnitude

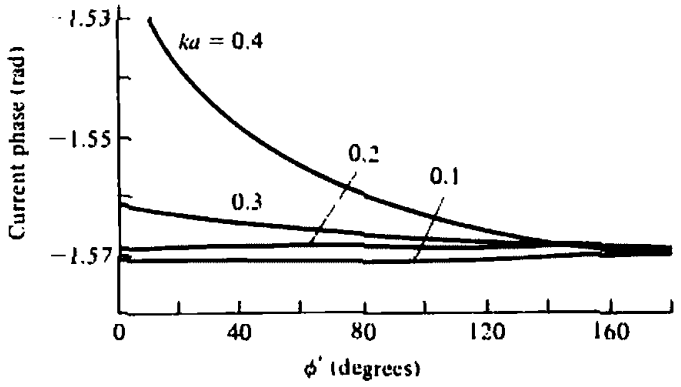

(b) Phase

Figure 5.9 Current magnitude and phase distributions on small circular loop antennas. (SOURCE: J. E. Storer, "Impedance of Thin-Wire Loop Antennas," *AIEE Trans.*, Vol. 75, November 1956. © 1956 IEEE)

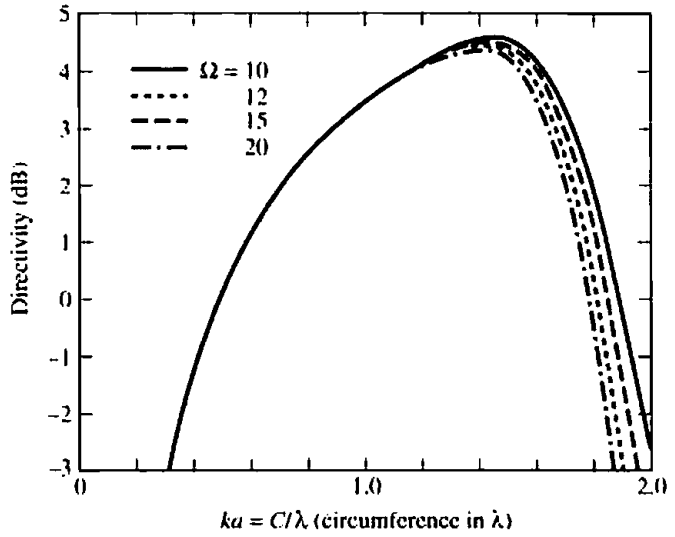

Figure 5.10 Directivity of circular-loop antenna for $\theta = 0, \pi$ versus electrical size (circumference/wavelength). (SOURCE: G. S. Smith, "Loop Antennas," copyright © McGraw-Hill, Inc. Permission by McGraw-Hill, Inc.)

$= 0.1, 0.2, 0.3$, and 0.4 and the wire size was chosen so that $\Omega = 2 \ln(2\pi a/b) = 10$. It is apparent that for $ka = 0.1$ the current is nearly uniform. For $ka = 0.2$ the variations are slightly greater and become even larger as ka increases. On the basis of these results, loops much larger than $ka = 0.2$ (radius much greater than 0.03–0.04λ) cannot be considered small.

As was indicated earlier, the maximum of the pattern for a loop antenna shifts from the plane of the loop ($\theta = 90°$) to its axis ($\theta = 0°, 180°$) as the circumference of the loop approaches one wavelength. Based on the nonuniform current distribution of (5-67), the directivity of the loop along $\theta = 0°$ has been computed, and it is plotted in Figure 5.10 versus the circumference of the loop in wavelengths [5]. The maximum directivity is about 4.5 dB, and it occurs when the circumference is about 1.4λ. For a one wavelength circumference, which is usually the optimum design for a helical antenna, the directivity is about 3.4 dB. It is also apparent that the directivity is basically independent of the radius of the wire, as long as the circumference is equal or less than about 1.3 wavelengths; there are differences in directivity as a function of the wire radius for greater circumferences.

Computed impedances, based on the Fourier series representation of the current, are shown plotted in Figure 5.11. The input resistance and reactance are plotted as a function of the circumference C (in wavelengths) for $0 \leq ka = C/\lambda \leq 2.5$. The diameter of the wire was chosen so that $\Omega = 2 \ln(2\pi a/b) = 8, 9, 10, 11$, and 12. It is apparent that the first antiresonance occurs when the circumference of the loop is about $\lambda/2$, and it is extremely sharp. It is also noted that as the loop wire increases in thickness, there is a rapid disappearance of the resonances. As a matter of fact, for $\Omega < 9$ there is only one antiresonance point. These curves (for $C > \lambda$) are similar, both qualitatively and quantitatively, to those of a linear dipole. The major difference is that the loop is more capacitive (by about 130 ohms) than a dipole. This shift in reactance allows the dipole to have several resonances and antiresonances while moderately thick loops ($\Omega < 9$) have only one antiresonance. Also small loops are primarily inductive while small dipoles are primarily capacitive. The resistance curves for the loop and the dipole are very similar.

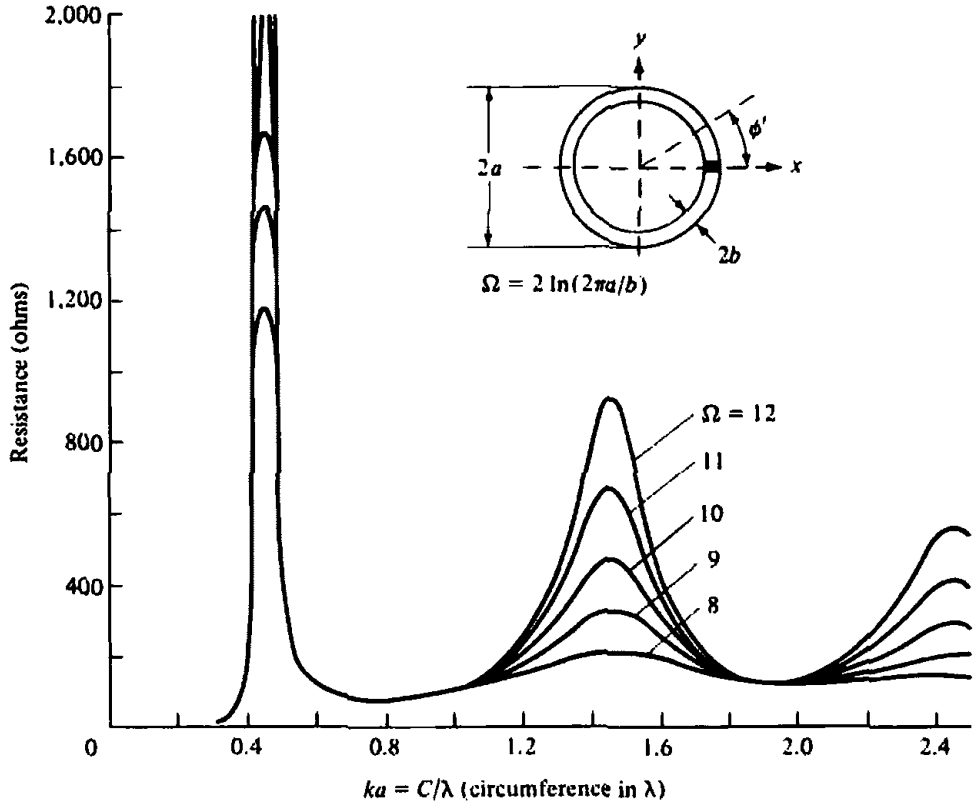

(a) Resistance

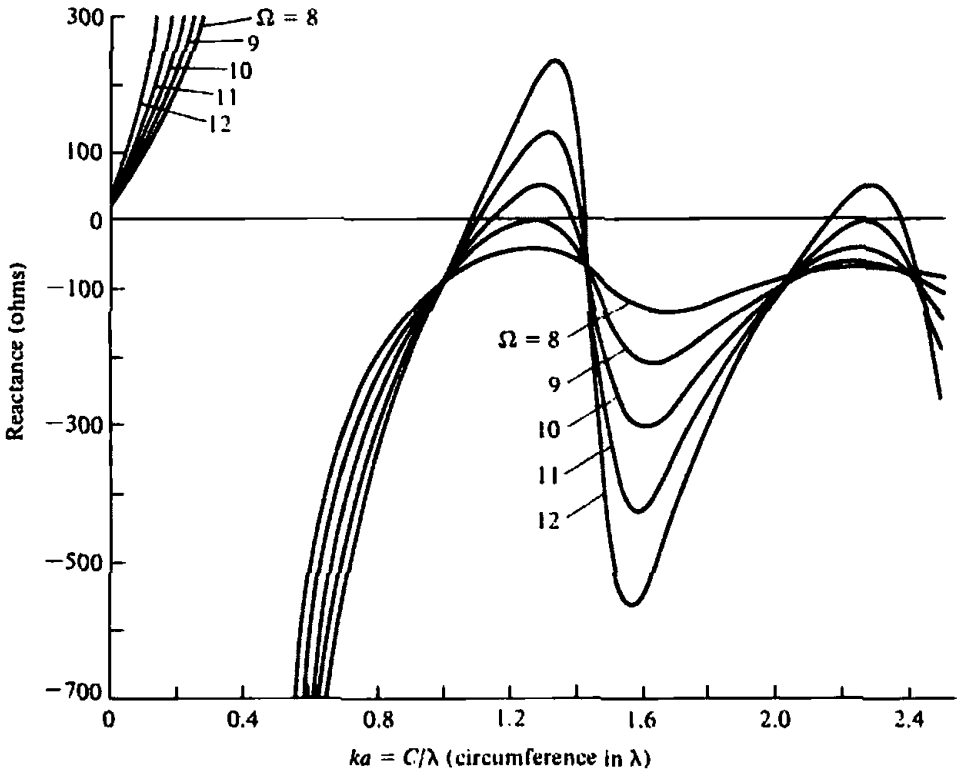

(b) Reactance

Figure 5.11 Input impedance of circular loop antennas. (SOURCE: J. E. Stover, "Impedance of Thin-Wire Loop Antennas," *AIEE Trans.*, Vol. 75, November 1956. © 1956 IEEE).

To verify the analytical formulations and the numerical computations, loop antennas were built and measurements of impedance were made [6]. The measurements were conducted using a half-loop over an image plane, and it was driven by a two-wire line. An excellent agreement between theory and experiment was indicated everywhere except near resonances where computed conductance curves were slightly higher than those measured. This is expected since ohmic losses were not taken into account in the analytical formulation. It was also noted that the measured susceptance curve was slightly displaced vertically by a constant value. This can be attributed to the "end effect" of the experimental feeding line and the "slice generator" used in the analytical modeling of the feed. For a dipole, the correction to the analytical model is usually a negative capacitance in shunt with the antenna [15]. A similar correction for the loop would result in a better agreement between the computed and measured susceptances. Computations for a half-loop above a ground plane were also performed by J. E. Jones [16] using the Moment Method.

The radiation resistance of a loop antenna, with a cosinusoidal current distribution, was computed [17] by evaluating triple integrals numerically. The results are shown in Figure 5.12 where they are compared with those of a uniform current distribution. It is evident that when the circumference of the loop is less than about 0.8λ, the constant current radiation resistances agree quite well with those of the cosinusoidal distribution.

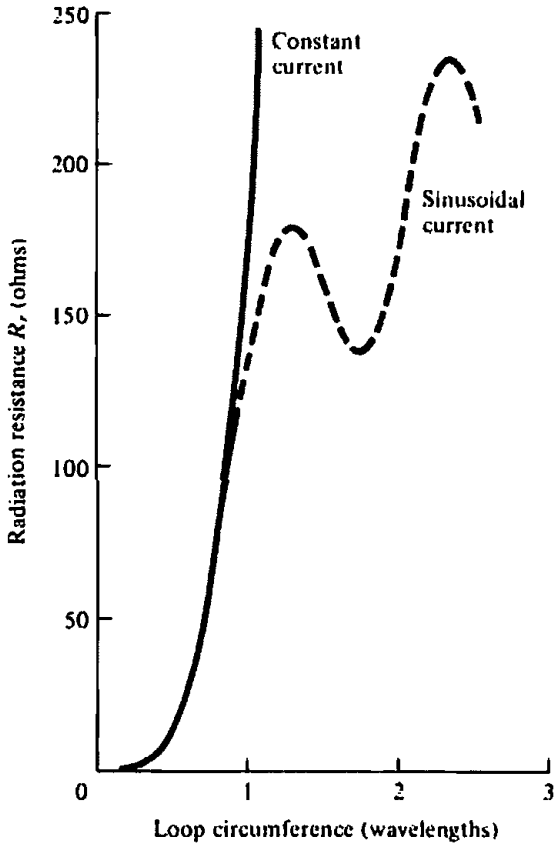

Figure 5.12 Radiation resistance of circular loop with constant and sinusoidal current distributions. (SOURCE: A. Richtscheid, "Calculation of the Radiation Resistance of Loop Antennas with Sinusoidal Current Distribution," *IEEE Trans. Antennas Propagat.*, Vol. AP-24, November 1976. © 1976 IEEE)

5.4.1 Arrays

In addition to be used as single elements, loop antennas are widely used in arrays. Two of the most popular arrays of loop antennas are the helical antenna and the Yagi-Uda array. The loop is also widely used to form a solenoid which in conjunction with a ferrite cylindrical rod within its circumference is used as a receiving antenna and as a tuning element, especially in transistor radios. This is discussed in Section 5.7.

The helical antenna, which is discussed in more detail in Section 10.3.1, is a wire antenna, which is wound in the form of a helix, as shown in Figure 10.13. It is shown that it can be modeled approximately by a series of loops and vertical dipoles, as shown in Figure 10.14. The helical antenna possesses in general elliptical polarization, but it can be designed to achieve nearly circular polarization. There are two primary modes of operation for a helix, the normal mode and the axial mode. The helix operates in its normal mode when its overall length is small compared to the wavelength, and it has a pattern with a null along its axis and the maximum along the plane of the loop. This pattern (figure eight type in the elevation plane) is similar to that of a dipole or a small loop. The helix operates in the axial mode when the circumference of the loop is between $3/4\lambda < C < 4/3\lambda$ with an optimum design when the circumference is nearly one wavelength. When the circumference of the loop approaches one wavelength, the maximum of the pattern is along its axis. In addition, the phasing among the turns is such that overall the helix forms an end-fire antenna with attractive impedance and polarization characteristics. In general, the helix is a popular communication antenna in the VHF and UHF bands.

The Yagi-Uda antenna is primarily an array of linear dipoles with one element serving as the feed while the others act as parasitic. However this arrangement has been extended to include arrays of loop antennas, as shown in Figure 10.27. As for the helical antenna, in order for this array to perform as an endfire array, the circumference of each of the elements is near one wavelength. More details can be found in Section 10.3.4 and especially in [8]–[10]. A special case is the quad antenna which is very popular amongst ham radio operators. It consists of two square loops, one serving as the excitation while the other is acting as a reflector; there are no directors. The overall perimeter of each loop is one wavelength.

5.4.2 Design Procedure

The design of small loops is based on the equations for the radiation resistance (5-24), (5-24a), directivity (5-31), maximum effective aperture (5-32), resonance capacitance (5-35), resonance input impedance (5-36) and inductance (5-37a), (5-37b). In order to resonate the element, the capacitor C_r of Figure 5.3 is chosen based on (5-35) so as to cancel out the imaginary part of the input impedance Z_{in}.

For large loops with a nonuniform current distribution, the design is accomplished using the curves of Figure 5.10 for the axial directivity and those of Figure 5.11 for the impedance. To resonate the loop, usually a capacitor in parallel or an inductor in series is added, depending on the radius of the loop and that of the wire.

Example 5.4

Design a resonant loop antenna to operate at 100 MHz so that the pattern maximum is along the axis of the loop. Determine the radius of the loop and that of the wire (in

meters), the axial directivity (in dB), and the parallel lumped element (capacitor in parallel or inductor in series) that must be used in order to resonate the antenna.

SOLUTION

In order for the pattern maximum to be along the axis of the loop, the circumference of the loop must be large compared to the wavelength. Therefore the current distribution will be nonuniform. To accomplish this, Figure 5.11(a) should be used. There is not only one unique design which meets the specifications, but there are many designs that can accomplish the goal.

One design is to select a circumference where the loop is self-resonant, and there is no need for a resonant capacitor. For example, referring to Figure 5.11(b) and choosing an $\Omega = 12$, the circumference of the loop is nearly 1.125λ. Since the free-space wavelength at 100 MHz is 3 meters, then the circumference is

$$\text{circumference} \simeq 1.125(3) = 3.375 \text{ meters}$$

while the radius of the loop is

$$\text{radius} = a = \frac{3.375}{2\pi} = 0.5371 \text{ meters}$$

The radius of the wire is obtained using

$$\Omega = 12 = 2 \ln\left(\frac{2\pi a}{b}\right)$$

or

$$\frac{a}{b} = 64.2077$$

Therefore the radius of the wire is

$$b = \frac{a}{64.2077} = \frac{0.5371}{64.2077} = 0.8365 \text{ cm} = 8.365 \times 10^{-3} \text{ meters}$$

Using Figure 5.10, the axial directivity for this design is approximately 3.6 dB. Using Figure 5.11(a), the input impedance is approximately

$$Z_{in} = Z'_{in} \simeq 125 \text{ ohms}$$

Since the antenna chosen is self-resonant, there is no need for a lumped element to resonate the radiator.

Another design will be to use another circumference where the loop is not self resonant. This will necessitate the use of a capacitor C_r to resonate the antenna. This is left as an end of the chapter exercise.

5.5 GROUND AND EARTH CURVATURE EFFECTS FOR CIRCULAR LOOPS

The presence of a lossy medium can drastically alter the performance of a circular loop. The parameters mostly affected are the pattern, directivity, input impedance,

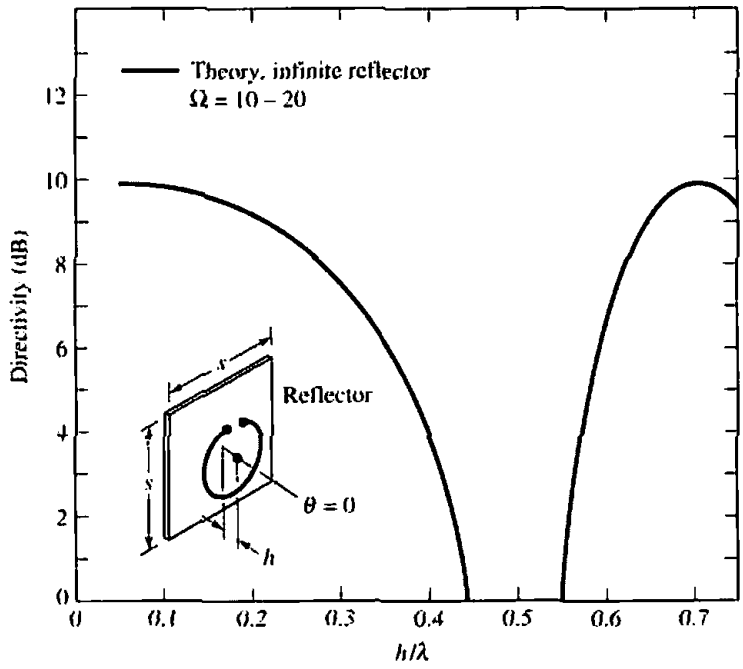

Figure 5.13 Directivity of circular-loop antenna, $C = ka \approx 1$, for $\theta = 0$ versus distance from reflector h/λ. Theoretical curve is for infinite planar reflector; measured points are for square reflector. (SOURCE: G. S. Smith, "Loop Antennas," copyright © McGraw-Hill, Inc. *Permission by McGraw-Hill, Inc.*)

and antenna efficiency. The amount of energy dissipated as heat by the lossy medium directly affects the antenna efficiency. As for the linear elements, geometrical optics techniques can be used to analyze the radiation characteristics of loops in the presence of conducting surfaces. The reflections are taken into account by introducing appropriate image (virtual) sources. Divergence factors are introduced to take into account the effects of the ground curvature. Because the techniques are identical to the formulations of Section 4.8, they will not be repeated here. The reader is directed to that section for the details. It should be pointed out, however, that a horizontal loop has horizontal polarization in contrast to the vertical polarization of a vertical electric dipole. Exact boundary-value solutions, based on Sommerfeld integral formulations, are available [16]. However they are too complex to be included in an introductory chapter.

By placing the loop above a reflector, the pattern is made unidirectional and the directivity is increased. To simplify the problem, initially the variations of the axial directivity ($\theta \approx 0°$) of a circular loop with a circumference of one wavelength ($ka = 1$) when placed horizontally a height h above an infinite in extent perfect electric conductor are examined as a function of the height above the ground plane. These were obtained using image theory and the array factor of two loops, and they are shown for $10 < \Omega < 20$ in Figure 5.13[5], [18]. Since only one curve is shown for $10 < \Omega < 20$, it is evident that the directivity variations as a function of the height are not strongly dependent on the radius of the wire of the loop. It is also apparent that for $0.05\lambda < h < 0.2\lambda$ and $0.65\lambda < h < 0.75\lambda$ the directivity is about 9 dB. For the same size loop, the corresponding variations of the impedance as a function of the height are shown in Figure 5.14[5], [18]. While the directivity variations are not strongly influenced by the radius of the wire, the variations of the impedance do show a dependence on the radius of the wire of the loop for $10 < \Omega < 20$.

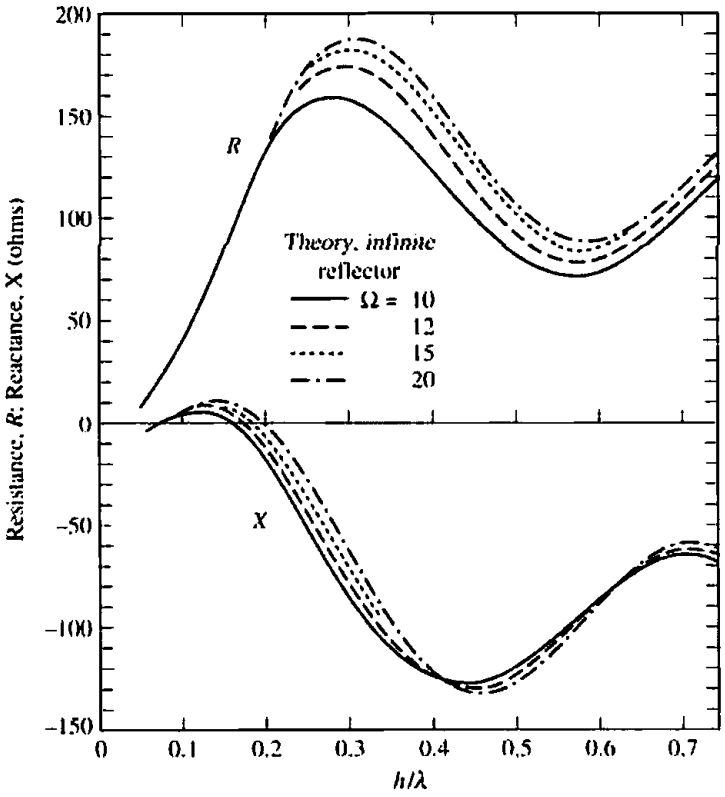

Figure 5.14 Input impedance of circular-loop antenna $C = ka = 1$ versus distance from reflector h/λ. Theoretical curves are for infinite planar reflector; measured points are for square reflector. (SOURCE: G. S. Smith, "Loop Antennas," copyright © 1984, McGraw-Hill, Inc. Permission by McGraw-Hill, Inc.)

A qualitative criterion that can be used to judge the antenna performance is the *ratio of the radiation resistance in free-space to that in the presence of the homogeneous lossy medium* [19]. This is a straightforward but very tedious approach. A much simpler method [20] is to find directly the self-impedance changes (real and imaginary) that result from the presence of the conducting medium.

Since a small horizontal circular loop is equivalent to a small vertical magnetic dipole (see Section 5.2.2), computations [21] were carried out for a vertical magnetic dipole placed a height h above a homogeneous lossy half-space. The changes in the self-impedance, normalized with respect to the free-space radiation resistance R_0 given by (5-24), are shown plotted in Figure 5.15. The parameter N_1 is defined by (4-124).

As for the vertical electric dipole, the magnitude changes of $\Delta R/R_0$ in Figure 5.15(a) approach unity as the height h of the antenna above a perfectly conducting ($|N_1^2| = \infty$) ground plane approaches zero ($2k_0h \to 0$). For the magnetic dipole (or the loop) this corresponds to a vanishing resistance. Also, as expected, the magnitude of ΔX approaches infinity as $2k_0h \to 0$. Both ΔR and ΔX become oscillatory as $2k_0h$ exceeds approximately π or when h exceeds about $\lambda_0/4$.

The effect the finite conductivity has on the resistance (ΔR) and reactance (ΔX) changes for $|N_1^2| = 100, 25, 4$ are shown in Figures 5.15(b) and (c). Significant modifications, compared to those of a perfect conductor, are indicated. The effects that a stratified lossy half-space have on the characteristics of a horizontal small circular loop have also been investigated and documented [22]. It was found that when a resonant loop is close to the interface, the changes in the input admittance as a function of the antenna height and the electrical properties of the lossy medium

were very pronounced. This suggests that a resonant loop can be used effectively to sense and to determine the electrical properties of an unknown geological structure.

5.6 POLYGONAL LOOP ANTENNAS

The most attractive polygonal loop antennas are the square, rectangular, triangular, and rhombic. These antennas can be used for practical applications such as for aircraft, missiles, and communications systems. However, because of their more complex structure, theoretical analyses seem to be unsuccessful [23]. Thus the application of these antennas has received much less attention. However design curves, computed using the Moment Method, do exist [24] and can be used to design polygonal loop antennas for practical applications. Usually the circular loop has been used in the UHF range because of its higher directivity while triangular and square loops have been applied in the HF and UHF bands because of advantages in their mechanical construction. Broadband impedance characteristics can be obtained from the different polygonal loops.

5.6.1 Square Loop

Next to the circular loop, the square loop is the simplest loop configuration. The far-field pattern for a small loop, in each of its principal planes, can be obtained by assuming that each of its sides is a small linear dipole of constant current I_0 and length l. Referring to Figure 5.16, the field in the y-z plane is given according to (4-26a) by

$$E_\phi = E_{\phi 1} + E_{\phi 2} = -j\eta \frac{kI_0 l}{4\pi}\left[\frac{e^{-jkr_1}}{r_1} - \frac{e^{-jkr_2}}{r_2}\right] \tag{5-68}$$

since the pattern of each element is omnidirectional in that plane. Using the far-field approximations of

$$\left.\begin{aligned} r_1 &\simeq r - \frac{l}{2}\sin\theta \\ r_2 &\simeq r + \frac{l}{2}\sin\theta \end{aligned}\right\} \quad \text{for phase variations} \tag{5-68a}$$

$$r_1 \simeq r_2 \simeq r \quad \text{for amplitude variations} \tag{5-68b}$$

(5-68) can be written as

$$E_\phi = \eta \frac{kI_0 l e^{-jkr}}{2\pi r}\sin\left(\frac{kl}{2}\sin\theta\right) \tag{5-69}$$

For small values of l ($l < \lambda/50$), (5-69) reduces to

$$\boxed{E_\phi = \eta \frac{(kl)^2 I_0 e^{-jkr}}{4\pi r}\sin\theta = \eta \frac{\pi S I_0 e^{-jkr}}{\lambda^2 r}\sin\theta} \tag{5-70}$$

where $S = l^2$ is the geometrical area of the loop. The corresponding magnetic field is given by

$$H_\theta = -\frac{E_\phi}{\eta} = -\frac{\pi S I_0 e^{-jkr}}{\lambda^2 r}\sin\theta \tag{5-71}$$

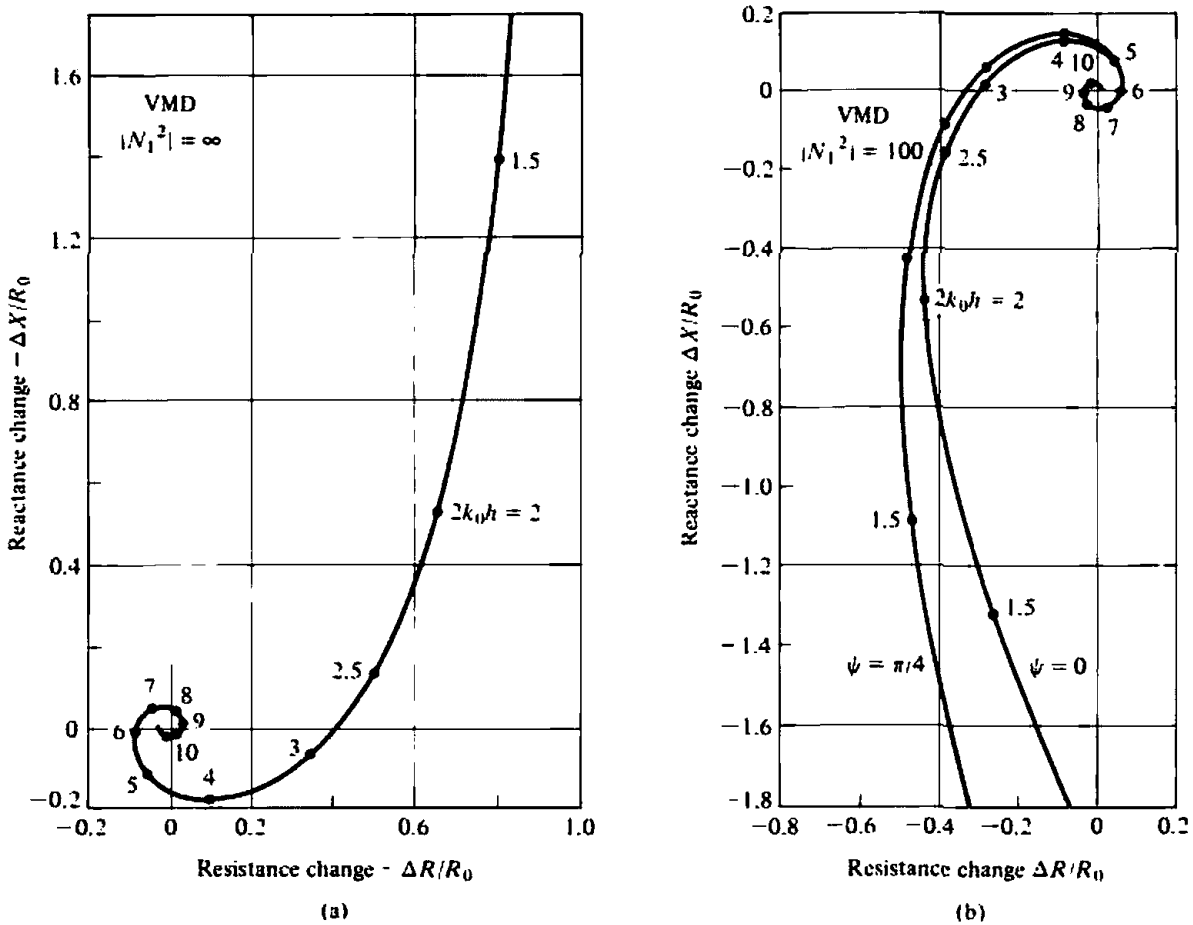

Figure 5.15 Vertical magnetic dipole (VMD) (or small horizontal loop) impedance change as a function of height above a homogeneous lossy half-space. (SOURCE: R. E. Collin and F. J. Zucker (eds.), *Antenna Theory Part 2*, McGraw-Hill, New York, 1969).

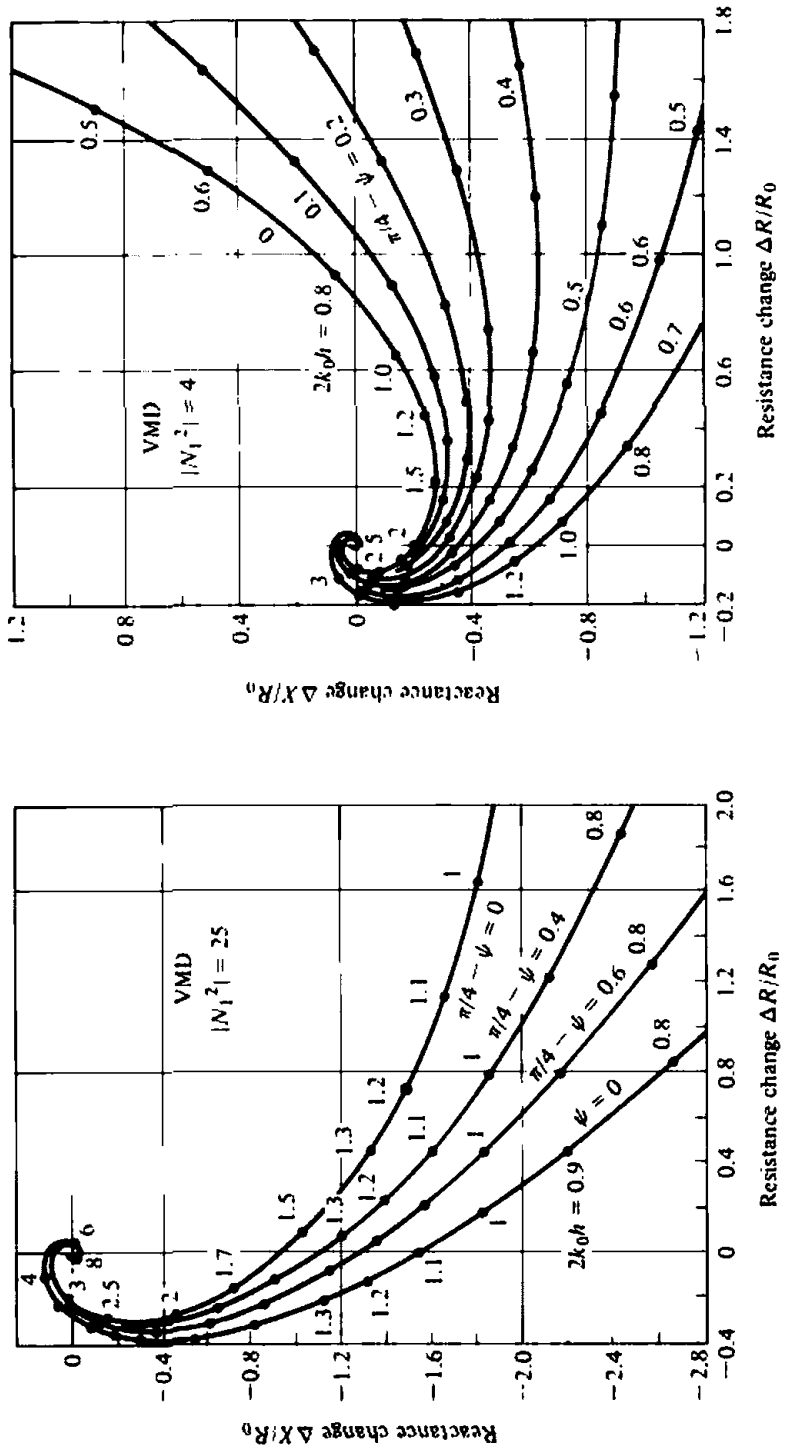

Figure 5.15 (continued)

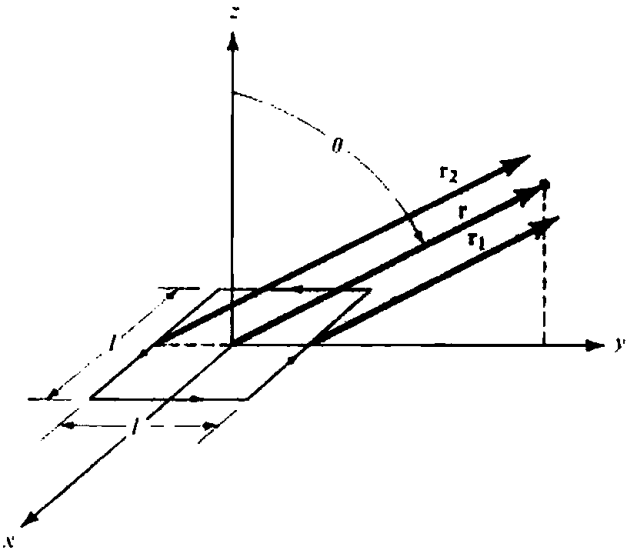

Figure 5.16 Square loop geometry for far-field observations on the y-z plane.

Equations (5-70) and (5-71) are identical to (5-27b) and (5-27a), respectively, for the small circular loop. Thus the far-zone principal-plane fields of a small square loop are identical to those of a small circular loop. The fields in the other planes are more difficult to obtain, and they will not be attempted here. However design curves are included which can be used for practical design applications.

5.6.2 Triangular, Rectangular, and Rhombic Loops

Shown in Figure 5.17 are the polygonal loops for which design data will be presented. They consist of top- and base-driven triangular loops, a rectangular loop, and a rhombic loop. The top-driven triangular loop has its feed at the top corner of the isosceles triangle while the base-driven configuration has its terminals at the base. The rectangular loop has its feed at the center of one of its sides while the rhombic configuration has its terminals at one of its corners.

The parameter β defines the angle of the top corner of the isosceles triangle for the triangular and rhombic loops while $\gamma = W/H$ is used to identify the relative side dimensions of the rectangular loop. The perimeter of each loop is given by P; for the rectangular loop, $P = 2(H + W)$. For all configurations, the radius of the wire is b.

Shown in Figure 5.18 are the input impedance ($Z = R + jX$) variations, as a function of P (in wavelengths), of the four configurations shown in Figure 5.17. The interval between adjacent points on each curve is $\Delta P/\lambda = 0.2$. Depending on the parameters β or γ, the input resistance of polygonal loops near the resonance frequency changes drastically. The reactance goes to zero when a loop approaches a short-circuited $\lambda/2$ long transmission line. In design then, the shape of the loop can be chosen so that the input impedance is equal to the characteristic impedance of the transmission line. Although the curves in Figure 5.18 are for specific wire radii, the impedance variations of the polygonal antennas as a function of the wire diameter are similar to those of the dipole.

Because the radius of the impedance locus for the $\beta = 60°$ of the top-driven triangular loop [Figure 5.18(a)] is smaller than for the other values of β, the $\beta = 60°$

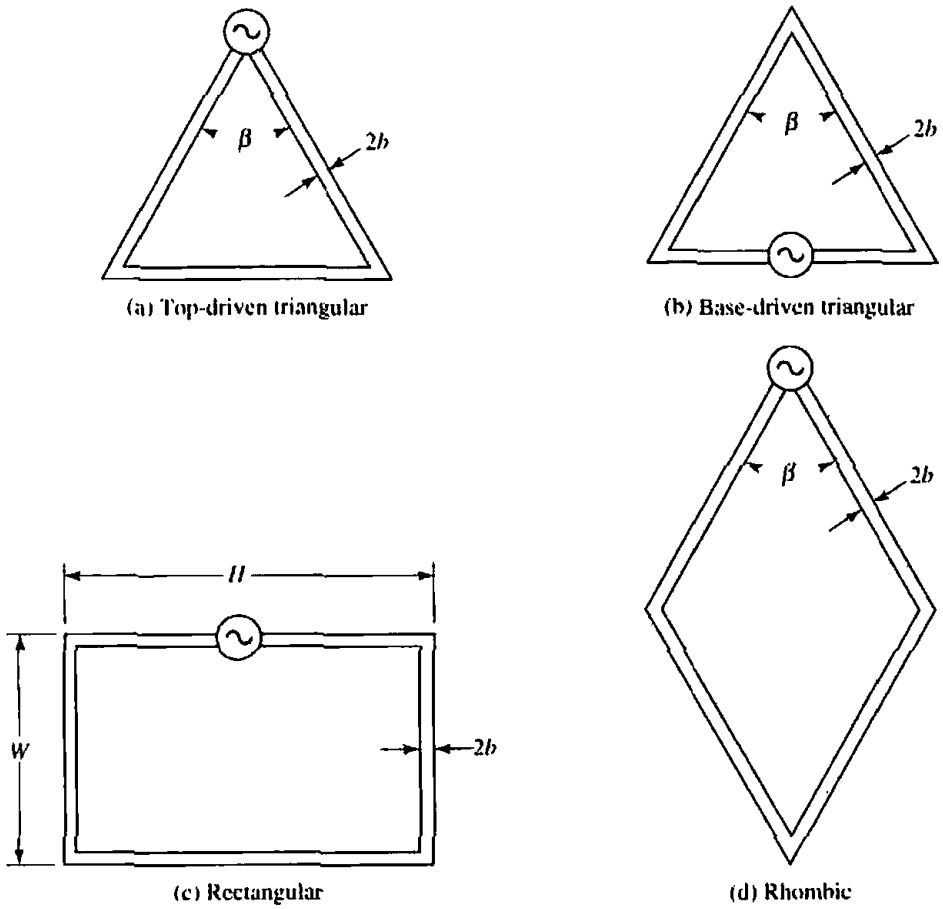

Figure 5.17 Typical configurations of polygonal loop antennas. (SOURCE: T. Tsukiji and S. Tou, "On Polygonal Loop Antennas," *IEEE Trans. Antennas Propagat.*, Vol. AP-28, No. 4, July 1980. © 1980 IEEE)

has the broadest impedance bandwidth compared with other triangular shapes or with the same shape but different feed points. Similar broadband impedance characteristics are indicated in Figure 5.18(c) for a rectangular loop with $\gamma = 0.5$ (the side with the feed point is twice as large as the other).

It can then be concluded that if the proper shape and feed point are chosen, a polygonal loop can have broadband impedance characteristics. The most attractive are the top-driven triangular loop with $\beta = 60°$ and the rectangular loop with $\gamma \approx 0.5$. A 50–70 ohm coaxial cable can be matched with a triangular loop with $\beta \approx 40°$. Rectangular loops with greater directivities, but with less ideal impedance characteristics, are those with larger values of γ.

The frequency characteristics of a polygonal loop can be estimated by inspecting its current distribution. When the current standing wave pattern has, at its antiresonant frequency, a null at a sharp corner of the loop, the loop has a very low current standing wave and, hence, broadband impedance characteristics.

Radiation patterns for the $\beta = 60°$ top- and base-driven triangular loops and the $\gamma = 4$ rectangular loop, for various values of P (in wavelengths), were also computed [24]. It was noted that for low frequencies near the resonance, the patterns of the top- and base-driven triangular loops were not too different. However, for higher frequencies the base-driven triangular loop had a greater gain than its corresponding top-driven configuration. In general, rectangular loops with larger γ's have greater gains.

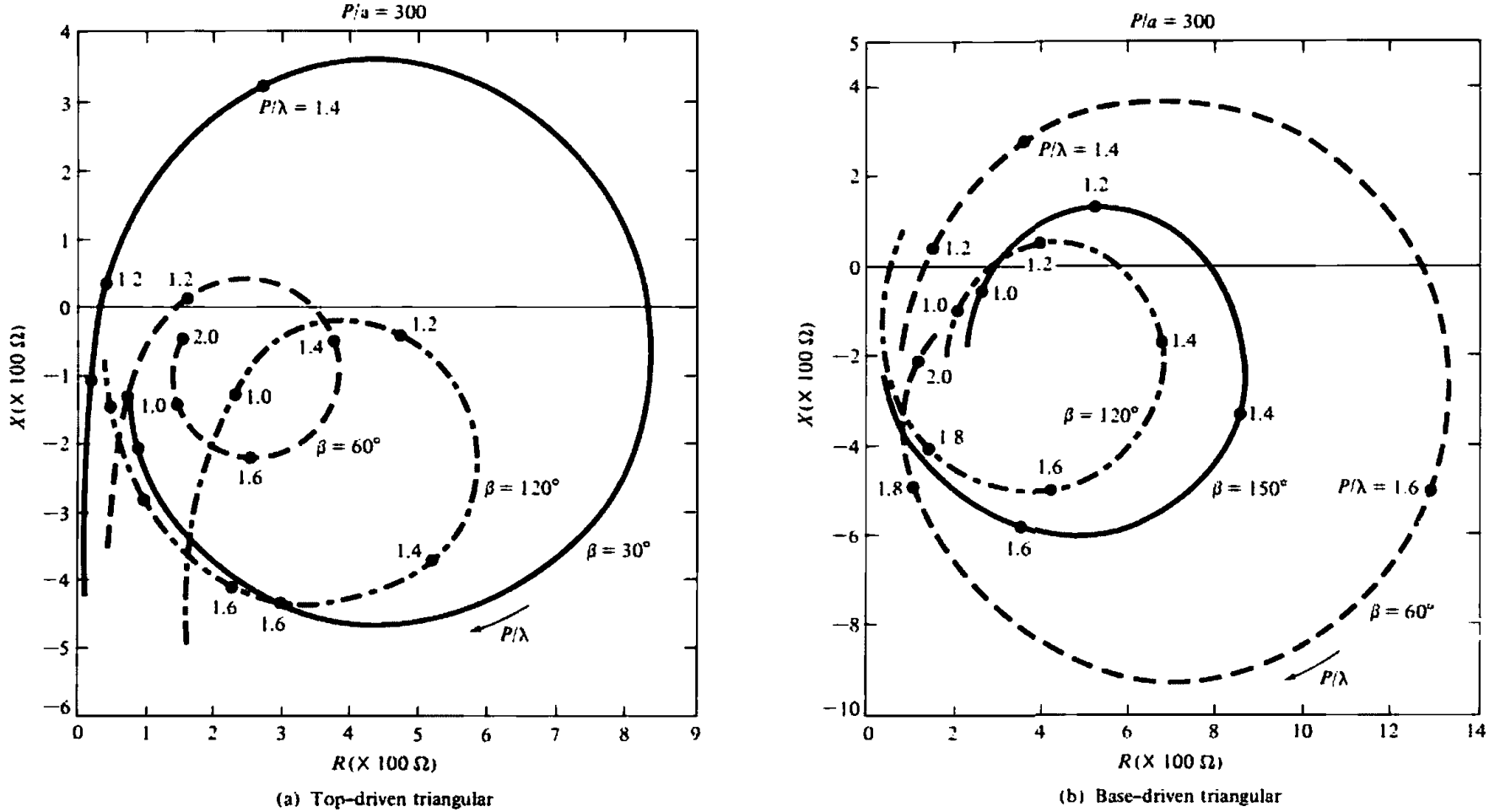

(a) Top-driven triangular

(b) Base-driven triangular

Figure 5.18 Input impedances of polygonal loop antennas. (SOURCE: T. Tsukiji and S. Tou, "On Polygonal Loop Antennas," *IEEE Trans. Antennas Propagat.*, Vol. AP-28, No. 4, July 1980, © 1980 IEEE)

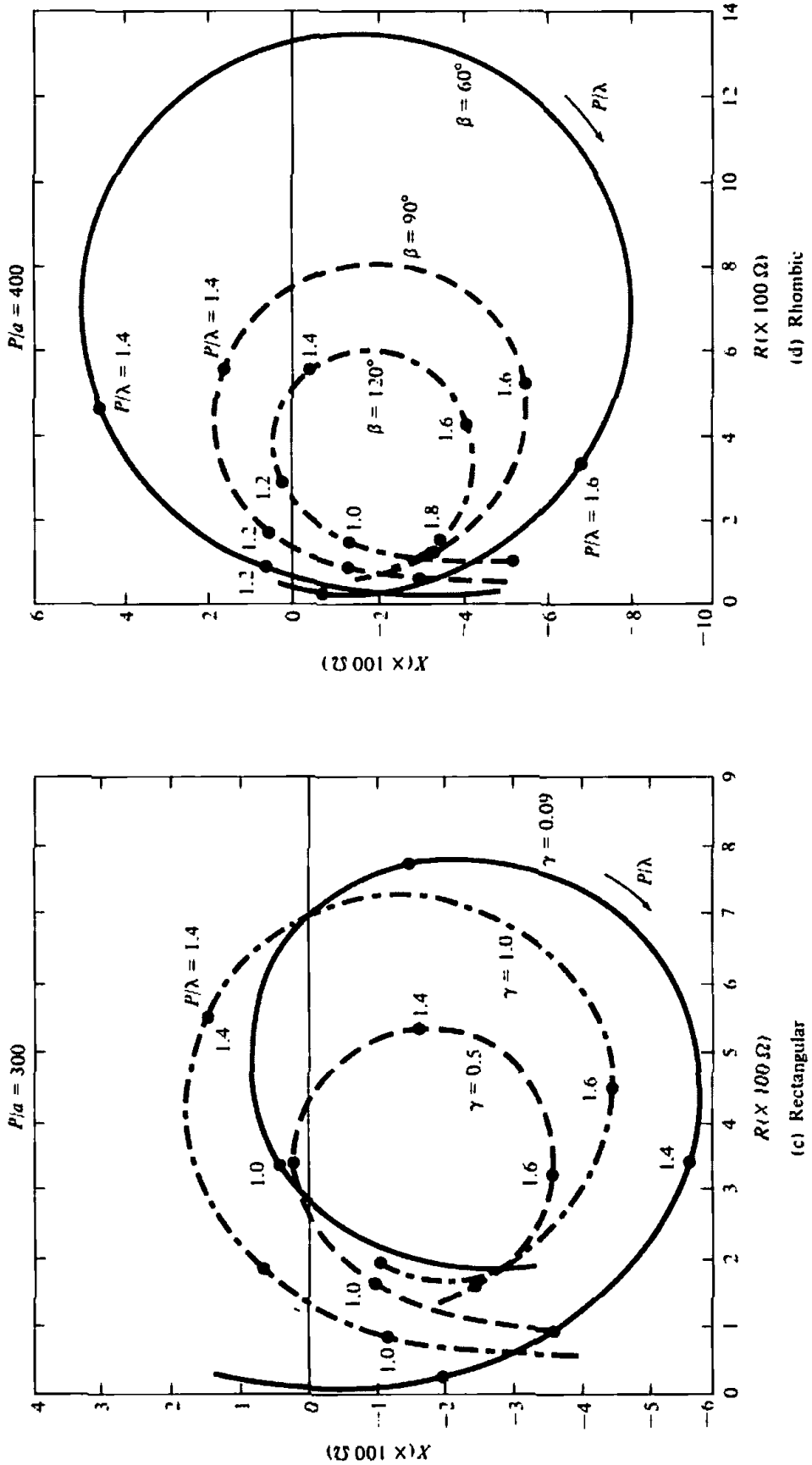

Figure 5.18 (continued)

5.7 FERRITE LOOP

Because the loss resistance is comparable to the radiation resistance, electrically small loops are very poor radiators and are seldom used in the transmitting mode. However, they are often used for receiving signals, such as in radios and pagers, where the signal-to-noise ratio is much more important than the efficiency.

5.7.1 Radiation Resistance

The radiation resistance, and in turn the antenna efficiency, can be raised by increasing the circumference of the loop. Another way to increase the radiation resistance, without increasing the electrical dimensions of the antenna, would be to insert within its circumference a ferrite core that has a tendency to increase the magnetic flux, the magnetic field, the open-circuit voltage, and in turn the radiation resistance of the loop [25]–[27]. This is the so-called *ferrite loop* and the ferrite material can be a rod of very few inches in length. The radiation resistance of the ferrite loop is given by

$$\frac{R_f}{R_r} = \left(\frac{\mu_{ce}}{\mu_0}\right)^2 = \mu_{cer}^2 \tag{5-72}$$

where

R_f = radiation resistance of ferrite loop
R_r = radiation resistance of air core loop
μ_{ce} = effective permeability of ferrite core
μ_0 = permeability of free-space
μ_{cer} = relative effective permeability of ferrite core

Using (5-24), the radiation resistance of (5-72) for a single-turn small ferrite loop can be written as

$$\boxed{R_f = 20\pi^2 \left(\frac{C}{\lambda}\right)^4 \left(\frac{\mu_{ce}}{\mu_0}\right)^2 = 20\pi^2 \left(\frac{C}{\lambda}\right)^2 \mu_{cer}^2} \tag{5-73}$$

and for an N-turn loop, using (5-24a), as

$$\boxed{R_f = 20\pi^2 \left(\frac{C}{\lambda}\right)^4 \left(\frac{\mu_{ce}}{\mu_0}\right)^2 N^2 = 20\pi^2 \left(\frac{C}{\lambda}\right)^4 \mu_{cer}^2 N^2} \tag{5-74}$$

The relative effective permeability of the ferrite core μ_{cer} is related to the relative intrinsic permeability of the unbounded ferrite material μ_{fr} ($\mu_{fr} = \mu_f/\mu_0$) by

$$\mu_{cer} = \frac{\mu_{ce}}{\mu_0} = \frac{\mu_{fr}}{1 + D(\mu_{fr} - 1)} \tag{5-75}$$

where D is the demagnetization factor which has been found experimentally for different core geometries, as shown in Figure 5.19. For most ferrite material, the relative intrinsic permeability μ_{fr} is very large ($\mu_{fr} \gg 1$) so that the relative effective permeability of the ferrite core μ_{cer} is approximately inversely proportional to the

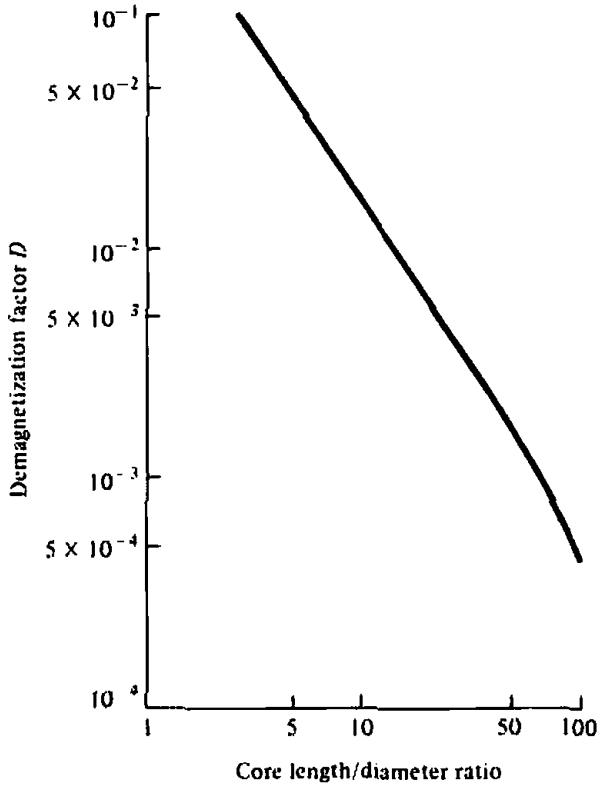

Figure 5.19 Demagnetization factor as a function of core length/diameter ratio. (SOURCE: E. A. Wolff, *Antenna Analysis*, Wiley, New York, 1966)

demagnetization factor, or $\mu_{rer} \sim 1/D = D'^{-1}$. In general, the demagnetization factor is a function of the geometry of the ferrite core. For example, the demagnetization factor for a sphere is $D = \frac{1}{3}$ while that for an ellipsoid of length $2l$ and radius a, such that $l \gg a$, is

$$D \approx \left(\frac{a}{l}\right)^2 \left[\ln\left(\frac{2l}{a}\right) - 1\right] \tag{5-75a}$$

5.7.2 Ferrite-Loaded Receiving Loop

Because of their smallness, ferrite loop antennas of few turns wound around a small ferrite rod are used as antennas especially in pocket transistor radios. The antenna is usually connected in parallel with the RF amplifier tuning capacitance and, in addition to acting as an antenna, it furnishes the necessary inductance to form a tuned circuit. Because the inductance is obtained with only few turns, the loss resistance is kept small. Thus the Q is usually very high, and it results in high selectivity and greater induced voltage.

The equivalent circuit for a ferrite loaded loop antenna is similar to that of Figure 5.3 except that a loss resistance R_M, in addition to R_L, is needed to account for the power losses in the ferrite core. Expressions for the loss resistance R_M and inductance L_A for the ferrite loaded loop of N turns can be found in [4] and depend on some empirical factors which are determined from an average of experimental results. The inductance L_i is the same as that of the unloaded loop.

5.8 MOBILE COMMUNICATION SYSTEMS APPLICATIONS

As was indicated in Section 4.7.4 of Chapter 4, the monopole is one of the most widely used elements for handheld units of mobile communication systems. An alternative to the monopole is the loop, [28]–[31], which has been often used in pagers but has found very few applications in handheld transceivers. This is probably due to loop's high resistance and inductive reactance which are more difficult to match to standard feed lines. The fact that loop antennas are more immune to noise makes them more attractive for an interfering and fading environment, like that of mobile communication systems. In addition, loop antennas become more viable candidates for wireless communication systems which utilize devices operating at higher frequency bands, particularly in designs where balanced amplifiers must interface with the antenna. Relative to top side of the handheld unit, such as the telephone, the loop can be placed either horizontally [29] or vertically [31]. Either configuration presents attractive radiation characteristics for land-based mobile systems.

References

1. E. H. Newman, P. Bohley, and C. H. Walter, "Two Methods for Measurement of Antenna Efficiency," *IEEE Trans. Antennas Propagat.*, Vol. AP-23, No. 4, July 1975, pp. 457–461.
2. G. S. Smith, "Radiation Efficiency of Electrically Small Multiturn Loop Antennas," *IEEE Trans. Antennas Propagat.*, Vol. AP-20, No. 5, September 1972, pp. 656–657.
3. G. S. Smith, "The Proximity Effect in Systems of Parallel Conductors," *J. Appl. Phys.*, Vol. 43, No. 5, May 1972, pp. 2196–2203.
4. J. D. Kraus, *Electromagnetics*, 4th ed., McGraw-Hill Book Co., New York, 1992.
5. G. S. Smith, "Loop Antennas," Chapter 5 in *Antenna Engineering Handbook*, second edition, McGraw-Hill Book Co., New York, 1984.
6. J. E. Storer, "Impedance of Thin-Wire Loop Antennas," *AIEE Trans.*, (Part I. Communication and Electronics), Vol. 75, Nov. 1956, pp. 606–619.
7. S. Adachi and Y. Mushiake, "Studies of Large Circular Loop Antenna," Sci. Rep. Research Institute of Tohoku University (RITU), B, 9, 2, 1957, pp. 79–103.
8. S. Ito, N. Inagaki, and T. Sekiguchi, "An Investigation of the Array of Circular-Loop Antennas," *IEEE Trans. Antennas Propagat.*, Vol. AP-19, No. 4, July 1971, pp. 469–476.
9. A. Shoamanesh and L. Shafai, "Properties of Coaxial Yagi Loop Arrays," *IEEE Trans. Antennas Propagat.*, Vol. AP-26, No. 4, pp. 547–550, July 1978.
10. A. Shoamanesh and L. Shafai, "Design Data for Coaxial Yagi Array of Circular Loops," *IEEE Trans. Antennas Propagat.*, Vol. AP-27, pp. 711–713, September 1979.
11. G. N. Watson, *A Treatise on the Theory of Bessel Functions*, Cambridge University Press, London, 1922.
12. J. E. Lindsay, Jr., "A Circular Loop Antenna with Non-Uniform Current Distribution," *IRE Trans. Antennas Propagat.*, Vol. AP-8, No. 4, July 1960, pp. 438–441.
13. E. A. Wolff, *Antenna Analysis*, Wiley, New York, 1966.
14. H. C. Pocklington, "Electrical Oscillations in Wire," *Cambridge Philosophical Society Proceedings*, London, England, Vol. 9, 1897, p. 324.
15. R. King, "Theory of Antennas Driven from Two-Wire Line," *Journal of Applied Physics*, Vol. 20, 1949, p. 832.
16. D. G. Fink (ed.), *Electronics Engineers' Handbook*, Section 18, "Antennas" (by W. F. Croswell), McGraw-Hill, New York, pp. 18–22.
17. A. Richtscheid, "Calculation of the Radiation Resistance of Loop Antennas with Sinu-

soidal Current Distribution," *IEEE Trans. Antennas Propagat.*, Vol. AP-24, No. 6, Nov. 1976, pp. 889–891.
18. K. Iizuka, R. W. P. King, and C. W. Harrison, Jr., "Self- and Mutual Admittances of Two Identical Circular Loop Antennas in a Conducting Medium and in Air," *IEEE Trans. Antennas Propagat.*, Vol. AP-14, No. 4, pp. 440–450, July 1966.
19. R. E. Collin and F. J. Zucher (eds.), *Antenna Theory Part 2*, Chapter 23 (by J. R. Wait), McGraw-Hill, New York, 1969.
20. J. R. Wait, "Possible Influence of the Ionosphere on the Impedance of a Ground-Based Antenna," *J. Res. Natl. Bur. Std.* (U.S.), Vol. 66D, September–October 1962, pp. 563–569.
21. L. E. Vogler and J. L. Noble, "Curves of Input Impedance Change Due to Ground for Dipole Antennas," *U.S. National Bureau of Standards, Monograph 72, January 31, 1964.*
22. D. C. Chang, "Characteristics of a Horizontal Circular Loop Antenna over a Multilayered, Dissipative Half-Space," *IEEE Trans. Antennas Propagat.*, Vol. AP-21, No. 6, November 1973, pp. 871–874.
23. R. W. P. King, "Theory of the Center-Driven Square Loop Antenna," *IRE Trans. Antennas Propagat.*, Vol. AP-4, No. 4, July 1956, p. 393.
24. T. Tsukiji and S. Tou, "On Polygonal Loop Antennas," *IEEE Trans. Antennas Propagat.*, Vol. AP-28, No. 4, July 1980, pp. 571–575.
25. M. A. Islam, "A Theoretical Treatment of Low-Frequency Loop Antennas with Permeable Cores," *IEEE Trans. Antennas Propagat.*, Vol. AP-11, No. 2, March 1963, pp. 162–169.
26. V. H. Rumsey and W. L. Weeks, "Electrically Small Ferrite Loaded Loop Antennas," *IRE Convention Record*, Vol. 4, Part 1, 1956, pp. 165–170.
27. E. A. Wolff, *Antenna Analysis*, Wiley, New York, 1966, pp. 75–89.
28. K. Fujimoto and J. R. James, *Mobile Antenna Systems Handbook*, Artech House, Norwood, MA, 1994.
29. M. A. Jensen and Y. Rahmat-Samii, "Performance Analysis of Antennas for Hand-Held Transceivers Using FDTD," *IEEE Trans. Antennas Propagat.*, Vol. 42, No. 8, pp. 1106–1113, August 1994.
30. M. A. Jensen and Y. Rahmat-Samii, "EM Interaction of Handset Antennas and a Human in Personal Communications," *Proc. IEEE*, Vol. 83, No. 1, pp. 7–17, January 1995.
31. C. A. Balanis, K. D. Katsibas and P. A. Tirkas, "Antenna Considerations for Wireless Communication Systems and Networks," Fifth International Conference on Advances in Communication and Control (ComCon 5), June 26–30, 1995, Rethymnon, Crete, Greece.

PROBLEMS

5.1. Derive
(a) (5-18a)–(5-18c) using (5-17) and (3-2a)
(b) (5-19a)–(5-19b) using (5-18a)–(5-18c)

5.2. Write the fields of an infinitesimal linear magnetic dipole of constant current I_m, length l, and positioned along the z-axis. Use the fields of an infinitesimal electric dipole, (4-8a)–(4-10c), and apply the principle of duality. Compare with (5-20a)–(5-20d).

5.3. Find the radiation efficiency of a single-turn and a 4-turn circular loop each of radius $\lambda/(10\pi)$ and operating at 10 MHz. The radius of the wire is $10^{-3}\lambda$ and the turns are spaced $3 \times 10^{-3}\lambda$ apart. Assume the wire is copper with a conductivity of 5.7×10^7 S/m, and the antenna is radiating into free-space.

5.4. Find the power radiated by a small loop by forming the average power density, using (5-27a)–(5-27c), and integrating over a sphere of radius r. Compare the answer with (5-23b).

5.5. For a small loop of constant current, derive its far-zone fields using (5-17) and the procedure outlined and relationships developed in Section 3.6. Compare the answers with (5-27a)–(5-27b).

5.6. Design a lossless resonant circular loop operating at 10 MHz so that its single turn radiation resistance is 0.73 ohms. The resonant loop is to be connected to a matched load through a balanced "twin-lead" 300-ohm transmission line.
(a) Determine the radius of the loop (in meters and wavelengths).
(b) To minimize the matching reflections between the resonant loop and the 300-ohm transmission line, determine the closest number of integer turns the loop must have.
(c) For the loop of part b, determine the maximum power that can be expected to be delivered to a receiver matched-load if the incident wave is polarization matched to the lossless resonant loop. The power density of the incident wave is 10^{-6} watts/m^2.

5.7. A resonant 6-turn loop of *closely spaced turns* is operating at 50 MHz. The radius of the loop is $\lambda/30$, and the loop is connected to a 50-ohm transmission line. The radius of the wire is $\lambda/300$, its conductivity is $\sigma = 5.7 \times 10^7$ S/m, and the spacing between the turns is $\lambda/100$. Determine the
(a) directivity of the antenna (in dB)
(b) radiation efficiency taking into account the proximity effects of the turns
(c) reflection efficiency
(d) gain of the antenna (in dB)

5.8. Find the radiation efficiency (in percent) of an 8-turn circular loop antenna operating at 30 MHz. The radius of each turn is $a = 15$ cm, the radius of the wire is $b = 1$ mm, and the spacing between turns is $2c = 3.6$ mm. Assume the wire is copper ($\sigma = 5.7 \times 10^7$ S/m), and the antenna is radiating into free space. Account for the *proximity effect*.

5.9. A very small circular loop of radius $a (a < \lambda/6\pi)$ and constant current I_0 is symmetrically placed about the origin at $x = 0$ and with the plane of its area parallel to the y-z plane. Find the
(a) spherical **E**- and **H**-field components radiated by the loop in the far-zone
(b) directivity of the antenna

5.10. Repeat Problem 5.9 when the plane of the loop is parallel to the x-z plane at $y = 0$.

5.11. Using the computer program at the end of this chapter, compute the radiation resistance and the directivity of a circular loop of constant current with a radius of
(a) $a = \lambda/50$ (b) $a = \lambda/10$
(c) $a = \lambda/4$ (d) $a = \lambda/2$

5.12. A constant current circular loop of radius $a = 5\lambda/4$ is placed on the x-y plane. Find the *two* smallest angles (excluding $\theta = 0°$) where a null is formed in the far-field pattern.

5.13. Design a circular loop of constant current such that its field intensity vanishes only at $\theta = 0°$ ($\theta = 180°$) and 90°. Find its
(a) radius
(b) radiation resistance
(c) directivity

5.14. Design a constant current circular loop so that its first minimum, aside from $\theta = 0°$, in its far-field pattern is at 30° from a normal to the plane of the loop. Find the
(a) smallest radius of the antenna (in wavelengths)
(b) relative (to the maximum) radiation intensity (in dB) in the plane of the loop

5.15. Design a constant current circular loop so that its pattern has a null in the plane of the loop, and two nulls above and two nulls below the plane of the loop. Find the
(a) radius of the loop
(b) angles where the nulls occur

5.16. *A constant current circular loop is placed on the x-y plane. Find the far-field position,* relative to that of the loop, that a linearly polarized probe antenna must have so that the polarization loss factor (PLF) is maximized.

5.17. A very small ($a \ll \lambda$) circular loop of constant current is placed a distance h above an infinite electric ground plane. Assuming z is perpendicular to the ground plane, find the total far-zone field radiated by the loop when its plane is parallel to the
(a) x-z plane
(b) y-z plane

5.18. A very small loop antenna ($a \ll \lambda/30$) of constant current is placed a height h above a flat, perfectly conducting ground plane of infinite extent. The area plane of the loop is parallel to the interface (x-y plane). For far-field observations
(a) find the total electric field radiated by the loop in the presence of the ground plane
(b) all the angles (in degrees) from the vertical to the interface where the total field will vanish when the height is λ
(c) the smallest nonzero height (in λ) such that the total far-zone field exhibits a null at an angle of 60° from the vertical

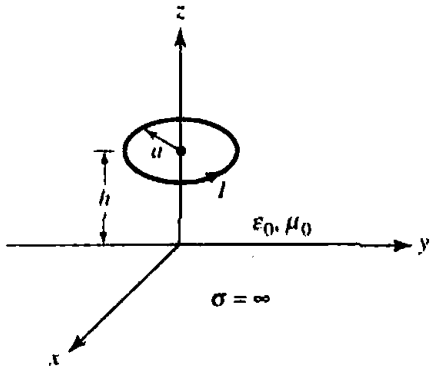

5.19. A small circular loop, with its area parallel to the x-z plane, is placed a height h above an infinite flat perfectly electric conducting ground plane. Determine
(a) the array factor for the equivalent problem which allows you to find the total field on and above the ground plane
(b) angle(s) θ (in degrees) where the array factor will vanish when the loop is placed at a height $\lambda/2$ above the ground plane

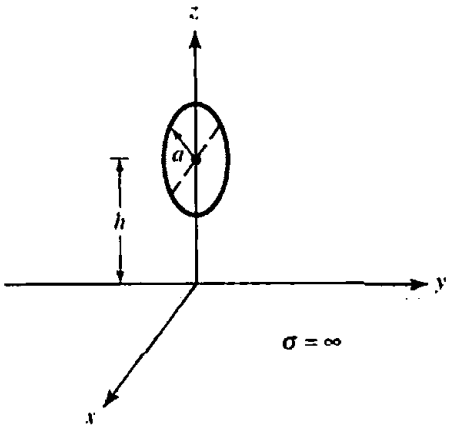

5.20. For the loop of Problem 5.17(a), find the smallest height h so that a null is formed in the y-z plane at an angle of 45° above the ground plane.

5.21. A small single-turn circular loop of radius $a = 0.05\lambda$ is operating at 300 MHz. Assuming the radius of the wire is $10^{-4}\lambda$, determine the
(a) loss resistance
(b) radiation resistance
(c) loop inductance
Show that the loop inductive reactance is much greater than the loss resistance and radiation resistance indicating that a small loop acts primarily as an inductor.

5.22. Determine the radiation resistance of a single-turn small loop, assuming the geometrical shape of the loop is
(a) rectangular with dimensions a and b ($a, b \ll \lambda$)
(b) elliptical with major axis a and minor axis b ($a, b, \ll \lambda$)

5.23. Show that for the rectangular loop the radiation resistance is represented by

$$R_r = 31.171 \left(\frac{a^2b^2}{\lambda^4}\right)$$

while for the elliptical loop is represented by

$$R_r = 31.171 \left(\frac{\pi^2a^2b^2}{16\lambda^4}\right)$$

Assuming the direction of the magnetic field of the incident plane wave coincides with the plane of incidence, derive the effective length of a small circular loop of radius a based on the definition of (2-92). Show that its effective length is

$$\mathbf{l}_e = \hat{\mathbf{a}}_\phi jkS \sin(\theta)$$

where $S = \pi a^2$.

5.24. A circular loop of nonconstant current distribution, with circumference of 1.4λ, is attached to a 300-ohm line. Assuming the radius of the wire is $1.555 \times 10^{-2}\lambda$, find the
(a) input impedance of the loop
(b) VSWR of the system
(c) inductance or capacitance that must be placed across the feed points so that the loop becomes resonant at $f = 100$ MHz

5.25. A very popular antenna for amateur radio operators is a square loop antenna (referred to as *quad antenna*) whose circumference is one wavelength. Assuming the radiation characteristics of the square loop are well represented by those of a circular loop:
(a) What is the input impedance (real and imaginary parts) of the antenna?
(b) What element (inductor or capacitor), and of what value, must be placed in series with the loop at the feed point to resonate the radiating element at a frequency of 1 GHz?
(c) What is the input VSWR, having the inductor or capacitor in place, if the loop is connected to a 78-ohm coaxial cable?

5.26. Design circular loops of wire radius b, which resonate at the first resonance. Find
(a) four values of a/b where the first resonance occurs (a is the radius of the loop)
(b) the circumference of the loops and the corresponding radii of the wires for the antennas of part (a)

5.27. Consider a circular loop of wire of radius a on the x–y plane and centered about the origin. Assume the current on the loop is given by

$$I_\phi(\phi') = I_0 \cos(\phi')$$

(a) Show that the far-zone electric field of the loop is given by

$$E_\theta \approx \frac{j\eta ka}{2} I_0 \frac{e^{-jkr}}{r} \frac{J_1(ka \sin \theta)}{ka \sin \theta} \cos \theta \sin \phi$$

$$E_\phi \approx \frac{j\eta ka}{2} I_0 \frac{e^{-jkr}}{r} J_1'(ka \sin \theta) \cos \phi$$

where

$$J_1'(x) = \frac{dJ_1(x)}{dx}$$

(b) Evaluate the radiation intensity $U(\theta, \phi)$ in the direction $\theta \approx 0$ and $\phi = \frac{\pi}{2}$ as a function of ka.

5.28. A very small circular loop, of constant current and radius of $\lambda_0/25$, is placed a height h above a perfect conductor and it is radiating in free-space.
(a) Find the smallest height h ($h < \lambda_0$) where the changes of its reactance are the smallest.
(b) At the height from part (a), find the radiation resistance of the loop.

5.29. A single-turn small loop of constant current I_0, radius $a = \lambda_0/(10\pi)$, and wire radius $b = \lambda_0/(500\pi)$ is placed a height h above a lossy ground plane, with the plane of the loop parallel to the ground. Assuming the lossy medium is flat earth with a conductivity of $\sigma_1 = 10^{-4}$ S/m, relative permittivity (dielectric constant) of $\epsilon_{r1} = 4$, and an operating frequency of 1 GHz, find the
(a) input resistance and reactance of the loop, assuming the wire of the loop is perfectly conducting and the loop is radiating in air (neglect ground effects)
(b) changes in the input resistance and input reactance when the loop is placed a height $h = 0.06\lambda_0$ above a flat, lossy earth
(c) total input resistance and input reactance when the loop is placed a distance $h = 0.06\lambda_0$ above a flat, lossy earth
(d) input reflection coefficient when the loop is connected to a 300-ohm "twin-lead" transmission line
(e) input VSWR when the loop is connected to the 300-ohm transmission line

COMPUTER PROGRAM - CIRCULAR LOOP

```
C*****************************************************************
C
C THIS IS A FORTRAN PROGRAM THAT COMPUTES THE:
C
C     I.  MAXIMUM DIRECTIVITY (DIMENSIONLESS AND IN dB)
C     II. RADIATION RESISTANCE
C
C FOR A SMALL (CONSTANT CURRENT) LOOP. THE LOOP IS
C RADIATING INTO FREE SPACE.
C
C THE DIRECTIVITY AND RADIATION RESISTANCE ARE
C CALCULATED USING THE TRAILING EDGE METHOD IN
C INCREMENTS OF 1° IN THETA.
C
C
C          **INPUT PARAMETERS
C          1. A: LOOP RADIUS (in wavelengths)
C
C          **NOTE
C          THE FAR-ZONE ELECTRIC FIELD COMPONENT E_φ
C          EXISTS FOR 0°≤ Θ ≤180° AND 0°≤ Φ ≤360°.
C
C
C*****************************************************************
```